Gliomes diffus de bas grade de sous type pédiatrique et tumeurs glio-neuronales "oligo-like" : caractérisation clinico-pathologique et moléculaire

Alice Metais

N° d'ordre : 40-2021- **ANNÉE 2021**

THÈSE D'EXERCICE / UNIVERSITÉ DE RENNES 1
sous le sceau de l'Université Bretagne Loire

Thèse en vue du

DIPLÔME D'ÉTAT DE DOCTEUR EN MÉDECINE

Présentée par

Alice METAIS

Née le 3 mai 1991 à Le Mans (72)

Challenges in the diagnosis of supratentorial tumors with an oligodendroglioma-like component occuring in children and young adults

Thèse soutenue à la Faculté de Médecine de Rennes
le 22 Avril 2021

devant le jury composé de :

Nathalie RIOUX-LECLERCQ
PU-PH, Anatomie et Cytologie Pathologique, CHU de Rennes / *Présidente du Jury*

Audrey ROUSSEAU
PU-PH, Anatomie et Cytologie Pathologiques, CHU Angers / E*xaminateur*

Pascale VARLET
PU-PH, Anatomie et Cytologie Pathologiques, GHU-Paris Sainte-Anne / E*xaminateur*

Laurent RIFFAUD
PU-PH, Neurochirurgie, CHU de Rennes / *Examinateur*

Pierre-Jean LE RESTE
PH, Neurochirurgie, CHU Rennes / Examinateur

Dominique FIGARELLA-BRANGER
PU-PH, Anatomie et Cytologie Pathologiques, CHU La Timone Marsseille / Directrice de thèse

N° d'ordre : 40-2021- **ANNÉE 2021**

UNIVERSITÉ DE RENNES 1

UNIVERSITE BRETAGNE LOIRE

THÈSE D'EXERCICE / UNIVERSITÉ DE RENNES 1
sous le sceau de l'Université Bretagne Loire

Thèse en vue du

DIPLÔME D'ÉTAT DE DOCTEUR EN MÉDECINE

Présentée par

Alice METAIS

Née le 3 mai 1991 à Le Mans (72)

Challenges in the diagnosis of supratentorial tumors with an oligodendroglioma-like component occuring in children and young adults

Thèse soutenue à la Faculté de Médecine de Rennes
le 22 Avril 2021

devant le jury composé de :

Nathalie RIOUX-LECLERCQ
PU-PH, Anatomie et Cytologie Pathologique, CHU de Rennes / *Présidente du Jury*

Audrey ROUSSEAU
PU-PH, Anatomie et Cytologie Pathologiques, CHU Angers / E*xaminateur*

Pascale VARLET
PU-PH, Anatomie et Cytologie Pathologiques, GHU-Paris Sainte-Anne / E*xaminateur*

Laurent RIFFAUD
PU-PH, Neurochirurgie, CHU de Rennes / *Examinateur*

Pierre-Jean LE RESTE
PH, Neurochirurgie, CHU Rennes / Examinateur

Dominique FIGARELLA-BRANGER
PU-PH, Anatomie et Cytologie Pathologiques, CHU La Timone Marsseille / Directrice de thèse

PROFESSEURS DES UNIVERSITES 2020

NOM	PRENOM	TITRE	SOUS-SECTION CNU
ANNE-GALIBERT	Marie-Dominique	PU-PH	Biochimie et biologie moléculaire
BARDOU-JACQUET	Edouard	PU-PH	Gastroentérologie ; hépatologie ; addictologie
BELAUD-ROTUREAU	Marc-Antoine	PU-PH	Histologie, embryologie et cytogénétique
BELLISSANT	Eric	PU-PH	Pharmacologie fondamentale ; pharmacologie clinique ; addictologie
BELOEIL	Hélène	PU-PH	Anesthésiologie-réanimation et médecine péri-opératoire
BENDAVID	Claude	PU-PH	Biochimie et biologie moléculaire
BENSALAH	Karim	PU-PH	Urologie
BEUCHEE	Alain	PU-PH	Pédiatrie
BONAN	Isabelle	PU-PH	Médecine physique et de réadaptation
BONNET	Fabrice	PU-PH	Endocrinologie, diabète et maladies métaboliques ; gynécologie médicale
BOUDJEMA	Karim	PU-PH	Chirurgie viscérale et digestive
BOUGET	Jacques	Professeur Emérite	Thérapeutique-médecine de la douleur ; addictologie
BOUGUEN	Guillaume	PU-PH	Gastroentérologie ; hépatologie ; addictologie
BRASSIER	Gilles	PU-PH	Neurochirurgie
BRETAGNE	Jean-François	Professeur Emérite	Gastroentérologie ; hépatologie ; addictologie
BRISSOT	Pierre	Professeur Emérite	Gastroentérologie ; hépatologie ; addictologie
CARRE	François	PU-PH	Physiologie
CATROS	Véronique	PU-PH	Biologie cellulaire
CATTOIR	Vincent	PU-PH	Bactériologie-virologie ; hygiène hospitalière
CHALES	Gérard	Professeur Emérite	Rhumatologie
CORBINEAU	Hervé	PU-PH	Chirurgie thoracique et cardiovasculaire
CUGGIA	Marc	PU-PH	Biostatistiques, informatique médicale et technologies de communication
DARNAULT	Pierre	PU-PH	Anatomie
DAUBERT	Claude	Professeur Emérite	Cardiologie
DAVID	Véronique	PU-PH	Biochimie et biologie moléculaire
DAYAN	Jacques	Professeur Emérite	Pédopsychiatrie ; addictologie
DE CREVOISIER	Renaud	PU-PH	Cancérologie ; radiothérapie
DECAUX	Olivier	PU-PH	Médecine interne ; gériatrie et biologie du vieillissement ; addictologie
DESRUES	Benoît	PU-PH	Pneumologie ; addictologie
DEUGNIER	Yves	Professeur Emérite	Gastroentérologie ; hépatologie ; addictologie
DONAL	Erwan	PU-PH	Cardiologie
DRAPIER	Dominique	PU-PH	Psychiatrie d'adultes ; addictologie
DUPUY	Alain	PU-PH	Dermato-vénérologie
ECOFFEY	Claude	PU-PH	Anesthésiologie-réanimation et médecine péri-opératoire
EDAN	Gilles	Professeur en surnombre	Neurologie
FERRE	Jean-Christophe	PU-PH	Radiologie et imagerie médicale
FEST	Thierry	PU-PH	Hématologie ; transfusion
FLECHER	Erwan	PU-PH	Chirurgie thoracique et cardiovasculaire
GANDEMER	Virginie	PU-PH	Pédiatrie
GANDON	Yves	PU-PH	Radiologie et imagerie médicale
GANGNEUX	Jean-Pierre	PU-PH	Parasitologie et mycologie
GARIN	Etienne	PU-PH	Biophysique et médecine nucléaire
GAUVRIT	Jean-Yves	PU-PH	Radiologie et imagerie médicale
GODEY	Benoît	PU-PH	Oto-rhino-laryngologie
GUGGENBUHL	Pascal	PU-PH	Rhumatologie
GUILLE	François	PU-PH	Urologie
GUYADER	Dominique	PU-PH	Gastroentérologie ; hépatologie ; addictologie
HAEGELEN	Claire	PU-PH	Anatomie
HOUOT	Roch	PU-PH	Hématologie ; transfusion
HUSSON	Jean Louis	Professeur Emérite	Chirurgie orthopédique et traumatologique
HUTEN	Denis	Professeur Emérite	Chirurgie orthopédique et traumatologique
JEGO	Patrick	PU-PH	Médecine interne ; gériatrie et biologie du vieillissement ; addictologie
JEGOUX	Franck	PU-PH	Oto-rhino-laryngologie
JOUNEAU	Stéphane	PU-PH	Pneumologie ; addictologie
KAYAL	Samer	PU-PH	Bactériologie-virologie ; hygiène hospitalière
LAMY DE LA CHAPELLE	Thierry	PU-PH	Hématologie ; transfusion

LAVIOLLE	Bruno	PU-PH	Pharmacologie fondamentale ; pharmacologie clinique ; addictologie
LAVOUE	Vincent	PU-PH	Gynécologie-obstétrique ; gynécologie médicale
LE BRETON	Hervé	PU-PH	Cardiologie
LE TULZO	Yves	PU-PH	Médecine intensive-réanimation
LECLERCQ	Christophe	PU-PH	Cardiologie
LEDERLIN	Mathieu	PU-PH	Radiologie et imagerie médicale
LEGUERRIER	Alain	Professeur Emérite	Chirurgie thoracique et cardiovasculaire
LEJEUNE	Florence	PU-PH	Biophysique et médecine nucléaire
LEVEQUE	Jean	PU-PH	Gynécologie-obstétrique ; gynécologie médicale
LIEVRE	Astrid	PU-PH	Gastroentérologie ; hépatologie ; addictologie
MABO	Philippe	PU-PH	Cardiologie
MAHE	Guillaume	PU-PH	Chirurgie vasculaire ; médecine vasculaire
MALLEDANT	Yannick	Professeur Emérite	Anesthésiologie-réanimation et médecine péri-opératoire
MATHIEU-SANQUER	Romain	PU-PH	Urologie
MENER	Eric	Professeur associé	Médecine générale
MEUNIER	Bernard	PU-PH	Chirurgie viscérale et digestive
MICHELET	Christian	Professeur Emérite	Maladies infectieuses ; maladies tropicales
MOIRAND	Romain	PU-PH	Gastroentérologie ; hépatologie ; addictologie
MORANDI	Xavier	PU-PH	Anatomie
MOREL	Vincent	Professeur associé	Médecine palliative
MOSSER	Jean	PU-PH	Biochimie et biologie moléculaire
MOURIAUX	Frédéric	PU-PH	Ophtalmologie
MYHIE	Didier	Professeur associé	Médecine générale
NAUDET	Florian	PU-PH	Thérapeutique-médecine de la douleur ; addictologie
ODENT	Sylvie	PU-PH	Génétique
OGER	Emmanuel	PU-PH	Pharmacologie fondamentale ; pharmacologie clinique ; addictologie
PARIS	Christophe	PU-PH	Médecine et santé au travail
PERDRIGER	Aleth	PU-PH	Rhumatologie
PLADYS	Patrick	PU-PH	Pédiatrie
RAVEL	Célia	PU-PH	Histologie, embryologie et cytogénétique
RENAUT	Pierric	Professeur associé	Médecine générale
REVEST	Matthieu	PU-PH	Maladies infectieuses ; maladies tropicales
RIFFAUD	Laurent	PU-PH	Neurochirurgie
RIOUX-LECLERCQ	Nathalie	PU-PH	Anatomie et cytologie pathologiques
ROBERT-GANGNEUX	Florence	PU-PH	Parasitologie et mycologie
ROPARS	Mickaël	PU-PH	Chirurgie orthopédique et traumatologique
SAINT-JAMES	Hervé	PU-PH	Biophysique et médecine nucléaire
SAULEAU	Paul	PU-PH	Physiologie
SEGUIN	Philippe	PU-PH	Anesthésiologie-réanimation et médecine péri-opératoire
SEMANA	Gilbert	PU-PH	Immunologie
SIPROUDHIS	Laurent	PU-PH	Gastroentérologie ; hépatologie ; addictologie
SOMME	Dominique	PU-PH	Médecine interne ; gériatrie et biologie du vieillissement ; addictologie
SOULAT	Louis	Professeur associé	Médecine d'urgence
SULPICE	Laurent	PU-PH	Chirurgie viscérale et digestive
TADIE	Jean Marc	PU-PH	Médecine intensive-réanimation
TARTE	Karin	PU-PH	Immunologie
TATTEVIN	Pierre	PU-PH	Maladies infectieuses ; maladies tropicales
THIBAULT	Ronan	PU-PH	Nutrition
THIBAULT	Vincent	PU-PH	Bactériologie-virologie ; hygiène hospitalière
THOMAZEAU	Hervé	PU-PH	Chirurgie orthopédique et traumatologique
TORDJMAN	Sylvie	PU-PH	Pédopsychiatrie ; addictologie
VERHOYE	Jean-Philippe	PU-PH	Chirurgie thoracique et cardiovasculaire
VERIN	Marc	PU-PH	Neurologie
VIEL	Jean-François	PU-PH	Epidémiologie, économie de la santé et prévention
VIGNEAU	Cécile	PU-PH	Néphrologie
VIOLAS	Philippe	PU-PH	Chirurgie infantile
WATIER	Eric	PU-PH	Chirurgie plastique, reconstructrice et esthétique ; brûlologie
WODEY	Eric	PU-PH	Anesthésiologie-réanimation et médecine péri-opératoire

MAITRES DE CONFERENCE DES UNIVERSITES 2020

NOM	PRENOM	TITRE	SOUS-SECTION CNU
ALLORY	Emmanuel	MCF associé	Médecine générale
AME-THOMAS	Patricia	MCU-PH	Immunologie
AMIOT	Laurence	MCU-PH	Hématologie ; transfusion
ANSELMI	Amédéo	MCU-PH	Chirurgie thoracique et cardiovasculaire
BANATRE	Agnès	MCF associé	Médecine générale
BEGUE	Jean Marc	MCU-PH	Physiologie
BERTHEUIL	Nicolas	MCU-PH	Chirurgie plastique, reconstructrice et esthétique ; brûlologie
BOUSSEMART	Lise	MCU-PH	Dermato-vénéréologie
BROCHARD	Charlène	MCU-PH	Physiologie
CABILLIC	Florian	MCU-PH	Biologie cellulaire
CASTELLI	Joël	MCU-PH	Cancérologie ; radiothérapie
CAUBET	Alain	MCU-PH	Médecine et santé au travail
CHAPRON	Anthony	MCF	Médecine générale
CHHOR-QUENIART	Sidonie	MCF associé	Médecine générale
CORVOL	Aline	MCU-PH	Médecine interne ; gériatrie et biologie du vieillissement ; addictologie
DAMERON	Olivier	MCF	Informatique
DE TAYRAC	Marie	MCU-PH	Biochimie et biologie moléculaire
DEGEILH	Brigitte	MCU-PH	Parasitologie et mycologie
DROITCOURT	Catherine	MCU-PH	Dermato-vénéréologie
DUBOURG	Christèle	MCU-PH	Biochimie et biologie moléculaire
DUGAY	Frédéric	MCU-PH	Histologie, embryologie et cytogénétique
EDELINE	Julien	MCU-PH	Cancérologie ; radiothérapie
FIQUET	Laure	MCF associé	Médecine générale
GANGLOFF	Cédric	MCF associé	Médecine d'urgence
GARLANTEZEC	Ronan	MCU-PH	Epidémiologie, économie de la santé et prévention
GOUIN épouse THIBAULT	Isabelle	MCU-PH	Hématologie ; transfusion
GUILLET	Benoit	MCU-PH	Hématologie ; transfusion
JAILLARD	Sylvie	MCU-PH	Histologie, embryologie et cytogénétique
KALADJI	Adrien	MCU-PH	Chirurgie vasculaire ; médecine vasculaire
KAMMERER-JACQUET	Solène-Florence	MCU-PH	Anatomie et cytologie pathologiques
LAVENU	Audrey	MCF	sciences physico-chimiques et ingénierie appliquée à la santé
LE GALL	François	MCU-PH	Anatomie et cytologie pathologiques
LEMAITRE	Florian	MCU-PH	Pharmacologie fondamentale ; pharmacologie clinique ; addictologie
MARTINS	Pédro Raphaël	MCU-PH	Cardiologie
MENARD	Cédric	MCU-PH	Immunologie
MICHEL	Laure	MCU-PH	Neurologie
MOREAU	Caroline	MCU-PH	Biochimie et biologie moléculaire
MOUSSOUNI	Fouzia	MCF	Informatique
PANGAULT	Céline	MCU-PH	Hématologie ; transfusion
ROBERT	Gabriel	MCU-PH	Psychiatrie d'adultes ; addictologie
SCHNELL	Frédéric	MCU-PH	Physiologie
THEAUDIN épouse SALIOU	Marie	MCU-PH	Neurologie
TURLIN	Bruno	MCU-PH	Anatomie et cytologie pathologiques
VERDIER épouse LORNE	Marie-Clémence	MCU-PH	Pharmacologie fondamentale ; pharmacologie clinique ; addictologie
ZIELINSKI	Agata	MCF	Philosophie

REMERCIEMENTS

A Madame le Professeur Nathalie Rioux-Leclercq, Professeure de Universités de Rennes 1 – Praticien Hospitalier, chef du service d'Anatomie et Cytologie Pathologiques, CHU Rennes, pour m'avoir fait l'honneur de présider mon jury de thèse, acceptez pour cela mes plus sincères remerciements. Toute ma reconnaissance également pour votre soutien tout au long de mon parcours.

A Madame le Professeur Pascale Varlet, Professeure des Universités de Paris – Praticien Hospitalier, service de Neuropathologie, GHU Paris Sainte-Anne, pour votre participation à ce jury et pour m'accueillir prochainement dans votre service.

A Madame le Professeur Audrey Rousseau, Professeure des Universités d'Angers – Praticien Hospitalier, département de Pathologie Cellulaire et Tissulaire, CHU Angers, pour votre participation à mon jury, pour votre accueil à Angers, vos enseignements, vos conseils et votre soutien.

A Monsieur le Professeur Laurent Riffaud, Professeur des Universités de Rennes 1-Praticien Hospitalier, service de Neurochirurgie, CHU Rennes, pour votre participation à mon jury, votre aide lors de la constitution de la cohorte que je présente aujourd'hui et votre accueil lors de mon semestre en neurochirurgie.

Au Docteur Pierre-Jean Le Reste, Praticien Hospitalier, service de Neurochirurgie, CHU Rennes, pour votre participation à mon jury, votre soutien et votre accueil bienveillant lors de mon semestre en neurochirurgie.

A Madame le Professeur Dominique Figarella-Branger, Professeure des Universités d'Aix-Marseille – Praticien Hospitalier, service d'Anatomie Pathologique et de Neuropathologie, CHU la Timone Marseille, pour m'avoir accueillie dans votre service et m'avoir donné l'opportunité de collaborer avec vous sur ce projet de recherche qui est devenue mon travail de thèse. Je vous remercie pour vos enseignements, votre direction efficace, votre disponibilité, vos conseils et votre soutien.

Je tiens à remercier les personnes qui ont participé à ce travail et l'ont rendu possible : l'équipe de biologie moléculaire de La Timone et en particulier Frédéric Fina et Catherine Gallardo pour les manipulations de digital PCR et le méthylome, Romain Appay pour ton encadrement bienveillant et ton aide, Carole Colin pour ton aide sur les statistiques et la rédaction, Emmanuelle Uro-Coste et son équipe pour la réalisation du RNAseq, Mélanie Pagès pour ton aide précieuse et efficace en bioinformatique, Sylvie Duclos et Karen Silva pour votre aide et vos astuces géniales, les membres du RENOCLIP pour nous avoir confié de si beaux cas.

Aux services d'Anatomie et Cytologie Pathologiques du CHU de Rennes et du CHBA de Vannes, pour les enseignements et l'expérience en pathologie générale que j'y ai reçu.

Au Département de Pathologie Cellulaire et Tissulaire du CHU d'Angers. Merci pour votre accueil chaleureux, votre bienveillance, et tout ce que vous m'avez transmis.

Au service d'Anatomie et Cytologie Pathologiques et de Neuropathologie du CHU La Timone Marseille. Merci également pour votre accueil ensoleillé, votre bienveillance, et tout ce que vous m'avez transmis.

Au service de Génétique Somatique des Cancers du CHU de Rennes pour cette première expérience de recherche qui m'a permis de valider mon Master 1 et m'a donné l'envie de poursuivre en Master 2.

Au service de Neurochirurgie du CHU de Rennes, pour cette expérience marquante dans mon internat. Merci pour l'expérience clinique et chirurgicale ainsi que les enseignements que j'y ai reçu.

Au service de Gastro-Entérologie de Saint-Malo pour l'expérience clinique dont j'ai bénéficié lors de mon stage.

A mes co-internes, de Saint-Malo, Rennes, Vannes, Angers, Marseille, pour leur amitié, leur soutien.

Au laboratoire OSS et à Eric Chevet pour son encadrement en Master 2, ses enseignements scientifiques, son soutien.

To my dear colleagues from OSS laboratory, and especially to Alexandra, Asia and Vesna.

Aux amis et aux copains de La Rochelle, de Poitiers, de Chamonix, d'Angers, de Marseille, de Rennes et d'ailleurs.

A ma famille, pour votre amour et votre soutien pendant ces longues années d'études.

A Estelle, ma sœur de cœur, pour ton amitié de toujours et ton soutien sans faille, pour les aventures ensembles passées et à venir.

A Massimo, per il tuo amore e supporto. Non vedo l'ora che questo nuovo capitolo insieme cominci. Il meglio deve ancora venire.

A Henri Cardon (1924-2015)

TABLE DES MATIERES

LISTE DES DOCUMENTS ANNEXES

LISTE DES ILLUSTRATIONS

LISTE DES ABREVIATIONS

BRAF: v-raf murine sarcoma viral oncogene homolog B

cIMPACT-NOW: Consortium to Inform Molecular and Practical Approaches to CNS Tumor taxonomy – Not Official WHO

CNA: copy number alteration

CNS: central nervous system

CNV: copy number variation

DN: dysplastic neurons

DNT: dysembryoplastic neuroepithelial tumor

EGFR: Epidermal Growth Factor Receptor

FA: fractional abundance

FAM: fluorescein

FFPE: formalin-fixed paraffin embedded

FGFR1-3: fibroblast growth factor receptor 1-3

GG: ganglioglioma

GNE: specific glioneuronal element

GNT: glioneuronal tumor

H3: Histone 3

HEX: hexachloro-6-carboxyfluorescein

HPS: hematoxylin-phloxin-saffron

IDH: isocitrate dehydrogenase

KCTD16: potassium channel tetramerization domain containing 16

KIAA1598: shootin 1

LEAT: long-term epilepsy associated tumors

MAPK: mitogen-associated protein kinase

MC: methylation class

mdPCR: multiplexed digital droplet PCR

MRI: magnetic resonance imaging

MYB: v-myb avian myeloblastosis viral oncogene homolog

MYBL1: v-myb avian myeloblastosis viral oncogene homolog-like 1

NOS: not otherwise specified

NPM1: nucleophosmin 1

NTRK: neurotrophic receptor tyrosine kinase

PCR: polymerase chain reaction

PLGG: paediatric-type low-grade glioma

PLNTY: polymorphous low-grade neuroepithelial tumor of the young

RAS: rat sarcoma viral oncogene homolog

RNA seq: RNA sequencing

RNF130: ring finger protein 130

TACC1-3: transforming acidic coiled-coil containing protein 1-3

TERT: telomerase reverse transcriptase

TKD: tyrosin kinase domain

TNS3: tensin 3

WHO: World health organization

Challenges in the diagnosis of supratentorial tumors with an oligodendroglioma-like component occurring in children and young adults

Alice Métais[1,2], Romain Appay[1,3]*, Mélanie Pagès[4]*, Catherine Gallardo[1], Karen Silva[5], Aurore Siegfried[6,7], Romain Perbet[8,9], Claude-Alain Maurage[8,9], Didier Scavarda[10], Frédéric Fina[1,11], Emmanuelle Uro-Coste[6,7], Laurent Riffaud[12,13], Carole Colin[3], Dominique Figarella-Branger[1,3] and contributors of the Biopathology RENOCLIP-LOC network

* Equally contributed

[1]APHM, CHU Timone, Service d'Anatomie Pathologique et de Neuropathologie, Marseille, France.

[2]Service d'Anatomie et Cytologie Pathologiques, CHU Pontchaillou, Rennes, France.

[3]Aix-Marseille Univ, CNRS, INP, Inst Neurophysiopathol, Marseille, France.

[4]GHU-Paris Sainte-Anne Hospital, Paris University, Paris, France.

[5]Groupe Hospitalier Est, Département de Neuropathologie, Hospices Civils de Lyon, Bron, France.

[6]Department of Pathological Anatomy and Histology-Cytology, Rangueil Hospital, Toulouse, France.

[7]Center for Research in Cancerology, Inserm U1037, University of Toulouse, Toulouse, France.

[8]Institute of Pathology, CHU Lille, Lille, France.

[9]LilNCog, Lille Neuroscience and Cognition, Univ. Lille, Inserm, CHU Lille, U1172, Lille,

France.

[10]Aix-Marseille Univ, APHM, Institut de Neurosciences des Systèmes, CHU Timone, Service de Neurochirurgie infantile, Marseille, France.

[11]ID Solutions, Research and Development, Grabels, France.

[12]Department of Pediatric Neurosurgery, Rennes University Hospital, Rennes, France.

[13]INSERM MediCIS, unit U1099 LTSI, Rennes 1 University, Rennes, France.

Biopathology RENOCLIP-LOC network: A. Rousseau (Angers), C. Godfraind (Clermont-Ferrand), C-A. Maurage (Lille), D. Meyronet (Lyon), G. Gauchotte (Nancy), F. Bielle (Paris), K. Mokhtari (Paris), P. Varlet (Paris), E. Uro-Coste (Toulouse), F. Vandenbos (Nice), G. Chotard (Bordeaux), F. Escande (Lille), Y. Nicaise (Toulouse).

ABSTRACT

Pediatric low-grade glial (PLGG) and glioneuronal tumors (GNT) are associated with drug-resistant epilepsy and occur in children and young adults. An oligodendroglioma-like component is a frequent feature of ganglioglioma (GG), dysembryoplasic neuropepithelial tumors (DNT) and in the two recently described entities: polymorphous low grade neuroepithelial tumor of the young (PLNTY) and diffuse LGG MAPK-altered. These tumors also share genetic alterations activating the MAPK kinase pathway. Therefore, they represent a diagnostic challenge.

We retrospectively studied 72 supratentorial LGG or GNT tumors with an oligodendroglioma-like component that we reclassified into three groups: GG (presence of dysplastic neurons, n=14), DNT (presence of glioneuronal element n=19) and GNT/PLGG (n=39). Targeted molecular analysis by multiplexed digital PCR (*BRAF*, *FGFR1* mutations and *FGFR1* duplication) found an alteration in 38/72 cases. Among the 34 cases without any alteration, RNA seq revealed a fusion transcript in 9/26. DNA-methylation profiling (n=46) found only 12 cases that displayed a calibrated score > 0.9 (26 %). Non informative calibrated score (> 0.3 and < 0.9) was observed in 26 cases (56.5%). In 8 cases calibrated score was less than 0.3 (17.5%). Unsupervised hierarchical clustering revealed 2 clusters in which GNT/PLGG tumors were equally distributed. LGG/GG cluster was enriched for histologically classified GG, *BRAF*V600E, CD34 expression and LGG GG methylation class (MC). LGG/DNT cluster was enriched for histologically classified DNT, *FGFR1* alterations, CD34 negative tumors and LGG DNT MC. Seven tumors fulfill diagnostic criteria for PLNTY. A decisional algorithm for histomolecular diagnosis of GG, DNT, PLNTY and LGG MAPK-altered is suggested.

Our study highlights the challenges in the diagnosis of supratentorial tumors with an oligodendroglioma-like component occurring in children and young adults and shows that these tumors belong to two major groups of biological relevance although four entities are currently recognized within this spectrum of tumors by WHO CNS5 classification.

INTRODUCTION

In 2016, the World Health Organization (WHO) classification of tumors of the CNS introduced for the first time molecular markers for the diagnosis of some entities (1). Accordingly, three major genetic alterations i.e. *H3* K27M mutation, *IDH* mutation and 1p19q codeletion stratify diffuse astrocytic and oligodendroglial tumors (2–4). As an example, both *IDH*-mutation and 1p19q codeletion are required to perform a diagnosis of oligodendroglioma and the terminology used for these tumors is now "(anaplastic) oligodendroglioma, *IDH*-mutant and 1p19q codeleted". However, gliomas, lacking *IDH* mutation or *H3* alterations, encompass a wide range of tumors that might display heterogeneous histological features, distinct genetic alteration and clinical behaviour according to the age of the patient. In 2016 a "pediatric box" was included in the chapter oligodendroglioma, *IDH*-mutant and 1p19q codeleted to describe a subgroup of gliomas recorded as "oligodendroglioma lacking *IDH* mutation and 1p19q codeletion (paediatric-type oligodendroglioma)" (1). These tumors mainly occured in children and adolescents and carry a good prognosis (5–7). The molecular landscape of these tumors has been recently described. Their tumorigenesis is driven by activation of the RAS-mitogen-activated protein kinase (RAS/MAPK) pathway, related to key genetic alterations in this signaling pathway (8–11). The cIMPACT-NOW group (*the consortium to Inform Molecular and Practical Approaches to CNS Tumor taxonomy*), has provided from a few years a forum to evaluate and recommend proposed changes to future CNS tumor classification (12). According to cIMPACT-NOW update 3, the terminology "diffuse astrocytic glioma, *IDH*-wild type with molecular features of glioblastoma, WHO grade IV " was introduced to describe a group of diffuse gliomas *IDH* wildtype appearing in elderly subjects associated with an aggressive clinical course and molecularly defined by gain of chromosome 7 and loss of chromosome 10 or *TERT* promoter mutation or *EGFR* amplification (13). This consortium has recently pointed out the molecular similarities between benign diffuse gliomas occurring in children and young adults and some other circumscribed gliomas and glioneuronal tumors, therefore introducing the concept of paediatric-type diffuse gliomas (14). They define this group as a WHO grade II infiltrating glioma with astrocytic and/or oligodendroglial differentiation, low or absent mitotic activity, absence of necrosis or microvascular proliferation and recurrent genetic alterations such as *BRAFV600E* mutation, *MYB* or *MYBL1* rearrangement, *FGFR1* alteration (15). The cIMPACT-NOW update 6 summarized the conclusions of the cIMPACT-Utrecht meeting and provide diagnostic

principle recommendations for the future CNS tumor classification and grading (16). Hence, the WHO CNS5 classification will change all WHO CNS tumor grades to Arabic numerals and diffuse gliomas will be divided into adult-type and pediatric-type (either low-grade or high-grade). Four tumor types are recorded in the group of pediatric-type diffuse low-grade gliomas: diffuse astrocytoma, *MYB* or *MYBL*-altered, angiocentric glioma, polymorphous low-grade neuroepithelial tumor of the young (PLNTY) and diffuse low grade glioma, MAPK-pathway-altered. Although diffuse astrocytoma, *MYB* or *MYBL*-altered, angiocentric glioma are characterized by an astrocytic component (17–19), polymorphous low-grade neuroepithelial tumor of the young (PLNTY) (20–25) and a subgroup of diffuse low grade glioma, MAPK-pathway-altered are characterized by a prominent oligodendroglioma-like component. This pattern is also shared by some glioneuronal tumors especially dysembryoplastic neuroepithelial tumor (DNT) and gangliоglioma (GG) (26). All these entities display genetic alterations in the MAPK-pathway. Although some recurrent genetic alterations are more frequent in some entities than in others it is obvious that two of them: the *BRAF* V600E mutation and *FGFR1* alterations have been reported in all of them and therefore diagnosis might be tricky in some cases.

Here we report a series of 72 supratentorial tumors occurring in paediatric setting and young adults characterized at histology by an obvious oligodendroglioma-like component associated or not with some characteristic pathological features leading to three major groups: gangliоglioma (GG, presence of dysplastic neurons), dysembryoplastic neuroepithelial tumors (DNT, characterized by the occurrence of the specific glioneuronal element) and a mixed group: glioneuronal tumors/pediatric low grade gliomas (GNT/PLGG). We performed careful clinic-pathological analysis, targeted molecular analysis by multiplexed digital PCR (*BRAF* mutation, *FGFR1* mutation and *FGFR1* duplication) and in a subset of cases DNA methylation profiling and RNA sequencing in order to define the most relevant pathological and molecular features of each group that could be instrumental in routine diagnostic practice to reach an integrated diagnosis according to the new CNS5 classification of brain tumors. Moreover, our results are discussed in line with the new entities recorded in the classification: the PLNTY and the group of diffuse low-grade gliomas, MAPK-pathway-altered.

MATERIALS

Tumor samples from 113 patients (from Rennes University Hospital, Marseille University Hospital, Lyon University Hospital, Lille University Hospital, Nice University Hospital, Grenoble University Hospital, GHU-Paris Sainte-Anne and Bordeaux University Hospital) operated on for a supratentorial tumor with a pathological diagnostic of dysembryoplastic neuroepithelial (DNT, simple, complex and non-specific form), ganglioglioma (GG), or glioneuronal tumor or paediatric-type low-grade glioma not otherwise specified (GNT/PLGG-NOS). Written informed consent to participate in this study was provided by the participants' legal guardian/next of kin. This study was reviewed and approved by the Aix-Marseille University ethics committee (2019-25-04-003). None of these cases displayed *IDH* mutation. All tissue samples were centrally reviewed (DFB, RA, AM) (Figure 1). Only tumors presenting with an oligodendroglioma-like component, associated or not with dysplastic neurons or a specific glioneuronal element (floating neurons in mucoid matrix) and one available formalin-fixed-paraffin embedded (FFPE) block were retained for further analysis, resulting in 72 cases effectively included in the study. Clinical and radiological data were retrospectively collected for each case. Clinical data included gender, tumor location, symptoms, age at first symptoms, age at surgery, extent of surgical resection, follow up (including date of last follow up and date of surgical excision for relapse if any), second resection if any. The delay between first and second resection was also recorded. Imaging was available for 59 patients. Minimal imaging data consisted in at least MRI report and if available significant FLAIR and T1 with gadolinium injection MRI sections.

METHODS

Pathological analysis and immunohistochemistry

Samples were stained with hematoxylin-phloxin-saffron (HPS) according to standard protocols. For each case the following pathological features were searched for and scored as present or absent: infiltrative growth pattern, nodular growth pattern, specific glioneuronal element (GNE), dysplatic neurons (DN), piloïd features, papillary features, rosette features, cytoplasmic vacuolization aspects, nuclei clustering, Rosenthal fibers, eosinophilic granular bodies, calcification, inflammation, siderophagous infiltrate, meningeal involvement, microvascular proliferation.

Immunochemistry was performed on Benchmark Ventana autostainer (Ventana Medical Systems SA, Illkirch, France) for OLIG2 (6F2, Dako®), CD34 (QBEnd10, Roche®), Neurofilament (2F11, Menarini®), Ki67 (MIB1, Dako®). In 36 cases BRAF immunostaining (VE1, Eurobio-Spring®) was also performed.

DNA extraction and quantification

DNA was extracted from each tumor samples (n=72) using the IDXTRACT-mag-FFPE kit (ID-Solutions, Grabels France) coupled to the automaton (IDEAL-32, ID-Solutions) as per the manufacturer's directions. DNA was qualified and quantified using DNA calibrated by an external standard range using the IDQUANTq kit (ID-Solutions) and the Mic® quantitative PCR instrument (Bio Molecular Systems, Queensland, Australia). If necessary, the DNA was diluted or concentrated (Vivacon 500, Sartorius Göttingen, Germany) in order to be able to perform a dPCR test sample of 8 µL of DNA in between 1 to 5 ng of DNA, and to have 250-500ng in 8µL. Technical steps for DNA extraction were performed in La Timone University hospital (Marseille) by CG. When insufficient DNA amount was extracted, additional sections were utilized. Post-scraping Hematoxylin-phloxin-saffron staining sections were systematically examined to ensure tumor cell content.

Multiplexed droplet digital PCR

BRAF V600E mutation, *BRAF* exon 14 duplication, *FGFR1* N546K and K656E mutations and *FGFR1* duplication were assessed for every patient of the cohort by multiplexed droplet digital PCR (mdPCR) as previously described (27–29). Technical steps for mdPCR were performed in La Timone University hospital (Marseille) by CG. Briefly, 8 µL of DNA comprising 1 to 5 ng and 13 µL of PCR mix (comprising uracil N-glycosylase (UNG), ready to use) were used for each mdPCR assay. A similar amplification program (50°C 2 min; 95°C 10 min; 40 x 95°C 30 sec- 60°C 1 min; 98°C 10 min) was used for all targets. The QX200 Droplet Digital PCR System (Bio-Rad) was used for the qualitative and quantitative analyses. The cut-off values and detection thresholds were set up as previously described (27–29). *BRAF* V600E mutation was targeted using 100% FAM labelled probe. *BRAF* exon 3, used as reference, was targeted using 100% HEX labelled probes. *BRAF* exon 14 was targeted using a mixture of both FAM and HEX labelled probes. *FGFR1* N546K and

K656E mutations were targeted using 100% FAM labelled probe, *FGFR1* exon 16 was targeted using 100% HEX labelled probes and *FGFR1* exon 8, used as reference, was targeted using a mixture of both FAM and HEX labelled probes. Fractional abundance (FA) and copy number variation (CNV) were calculated as described by Appay et al. 2020 (29).

Methylation analysis

Samples containing up to 250 ng DNA were selected for DNA methylation profiling. Technical steps were performed in La Timone University hospital (Marseille) by CG. DNA bisulfite conversion was processed using the ZymoEZ DNA methylation kit (Zymo research, USA), then treated with FFPE DNA Restore kit (Illumina, San Diego, CA, USA) and DNA clean and concentrator-5 (Zymo research, USA). The standard quality controls confirmed DNA quantity/quality and bisulfite conversion. The DNA was then processed using the Illumina Infinium HumanMethylation EPIC Bead-Chip array (Illumina, San Diego, CA, USA) according to the manufacturer's instructions. The iScan control software was used to generate raw data files from the BeadChip in IDAT format, analyzed using GenomeStudio version 2.0 (Illumina, San Diego, CA, USA) and were checked for quality measures according to the manufacturer's instructions.

Data processing

The .idat files were uploaded to the online CNS tumor DNA methylation classifier (11b4 version) at https://www.molecularneuropathology.org and a report for every tumor was generated, providing prediction scores for methylation classes (MC) and chromosomal copy-number plots. The calibrated scores were integrated to the histopathological findings according to the recommendations from Capper *et al*. (30,31). A methylation class (MC) associated with a calibrated score > 0.9 was relevant for diagnosis. A max-score between 0.3 and 0.9 was considered potentially useful but integrated with caution. No MC was given for a calibrated score less than 0.3.

Additional analyses were performed in R studio (v4.0.2). Raw signal intensities were obtained from .idat files using the minfi Bioconductor package (v1.34.0). Background correction and dye-bias correction were performed on each sample. Filtering criteria

of probes were removal of probes targeting X or Y chromosomes and removal of probes containing single nucleotide polymorphisms. Hierarchical clustering was performed using the Complex Heatmap package (2.4.3). Clustering of beta values from methylation arrays was performed based upon Euclidean distance with a ward algorithm. Methylation heatmap shows only the most variable probes (SD > 0.20). Tumors with a calibrated score for control tissue methylation classes were excluded.

RNA extraction and targeted RNA sequencing

Cases without alteration detected by mdPCR and for whom enough material was remaining underwent RNAseq analysis in Toulouse University Hospital (EUC, AS, YN) (32). RNA was extracted from two 8 microns thick FFPE material sections approximately, using the high Pure FFPE RNA Isolation Kit (catalogue # 06650775001, Roche diagnostics, Boulogne-Billancourt, France) according to the manufacturer's instruction.

The RNA concentrations were measured on a Qubit 4 Fluorometer (# Q33238, Thermo Fisher Scientific, USA) with the Invitrogen Qubit RNA BR Kit (# Q10210, Thermo Fisher Scientific). The percentage of RNA fragments >200 nt (fragment distribution value; DV200) was evaluated by capillary electrophoresis (Agilent 2100 Bioanalyzer). A DV200 >30% was required to process the next steps of analysis. NGS-based RNA sequencing was performed using the Illumina TruSight RNA Fusion Panel on a Nextseq550 instrument according to the manufacturer's instructions (Illumina, San Diego, CA, USA). This targeted RNA sequencing panel covers 507 fusion-associated genes, to assess most known cancer-related fusions. The TruSight RNA fusion panel gene list is available at https://www.illumina.com/content/dam/illumina-marketing/documents/products/gene_lists/gene_list_trusight_rna_fusion_panel.xlsx.

7690 exonic regions are targeted with 21 283 probes. Libraries were prepared according to Illumina's instructions of TruSight RNA fusion Panel kit. STAR_v2.6.1a or Bowtie softwares were used to produce aligned reads in relation to the Homo sapiens reference genome (UCSC hg19) (33). Manta v1.4.0, Tophat2 and Arriba tools were used for fusion calling (34).

Statistical analysis

Categorical variables were presented as frequencies and percentages, continuous variables as median and range or mean and standard deviation. The Fisher exact test was used to compare qualitative variables. Statistical tests were two-sided, the threshold for statistical significance was $p = 0.05$. Statistical analysis was done using XLSTAT software Version 2020.1.01 (Addinsoft, Paris, France).

RESULTS

Clinicopathological data

Seventy-two patients presenting with tumors with an oligo-like component were retained for further analysis after centralized histopathological review (figure 1). These include 39 women and 43 men (sex-ratio 1.43). Mean age at surgery was 18.4 +/- 12.4 years with 2 cases of infants (age ≤ 1 year) (2.8%), 42 cases of paediatric patients (age ranging from 1 year to 18 years) (58.3%) and 28 cases of adult patients (age above 18 years) (38.9%). Most of the cases (n = 63/72; 87.5%) had epilepsy, starting at a mean age of 15.5 +/- 10.9 years. Few cases presented neurological deficit (n = 3; 4.2%). Forty-nine cases had gross total resection (68%), 12 had biopsy or partial resection (16.7%) and information regarding surgical resection was not available for 11 patients (15.3%).

All tumors were supratentorial, most frequently localized in the temporal lobe (n=44; 61%), 12 in the frontal lobe (16.6 %), 4 in the parietal and 3 in the occipital. In 9 cases the tumor was localized in two or three lobes including the temporal lobe in 7/9. Altogether the temporal lobe was involved in 51 cases (70.8 %). Forty tumors demonstrated a cortical or cortico-subcortical localization (56%). Low signal T1 was observed in 40 cases (56%). High signal FLAIR was observed in 47 cases (65%). Contrast enhancement was observed in 30 cases (42%), edema in 5 cases (7%) and bubbly or cystic aspect in 31 cases (43%).

Follow-up data were available in 63 cases (87.5 %), with a median follow-up of 31.1 months [0-229.4 months]. Nine patients experimented recurrence associated with a second surgical resection, with a median time of 61.9 months [5.3-213.3 months] between the two interventions. No patient died. No patient had oncologic adjuvant therapy (radiotherapy or chemotherapy).

Among the 72 cases reviewed, 52 were initially diagnosed as DNT (either simple, complex or “non-specific form”, 72 %), 11 as GG (15%) and 9 as GNT/PLGG-NOS (13%). Central review board (DFB, RA, AM) reclassified each tumor in three groups: GG (presence of dysplastic neurons), DNT (presence of the specific GNE) or GNT/PLGG (oligodendroglioma-like component only associated or not with neuron-like component). Thus, 14 cases were reclassified as GG (19.5%), 19 cases were reclassified as DNT (26%) and 39 as GNT/PLGG (54.5%). In the whole cohort, infiltrative growth pattern was observed in 41 cases (57%) and nodular pattern was observed in 31 cases (43%). Meningeal involvement was observed in 21 cases (29%). Calcifications were recorded in 21 cases (29%), eosinophilic granular bodies in 16 cases (22%), Rosenthal fibers in 3 cases (4%), cytoplasmic vacuolization in 4 cases (5.5%), nucleus clustering in 7 cases (10%), inflammatory infiltrates in 14 cases (19%), piloïd features in 12 cases (17%), papillary features and rosette features in only 1 case (1.4%), siderophagous infiltrate in 7 cases (10%), and microvascular proliferation in 7 cases (10%). All tumors expressed OLIG2 and demonstrated residual axons with neurofilament staining. Mitotic activity was inconspicuous and Ki67 proliferation index was low (mean: 2.4% +/-3%). Extravascular CD34 immunostaining was present in 33 cases (46%).

Multiplex digital PCR

mdPCR was performed in all cases and demonstrated at least one alteration in 38 cases (53%) whereas no alteration was observed in 34 cases (47%). *FGFR1* alteration only was observed in 18 cases (25%) including 13 cases with *FGFR1* exon 16 duplication and 5 cases with *FGFR1* mutations. *BRAF* V600E mutation only was recorded in 18 cases (25%). Surprisingly, 2 cases presented with *FGFR1* exon 16 duplication associated to a *BRAF* V600E mutation. In these cases, BRAFV600E mutation was confirmed by immunohistochemistry. For further analyses these cases were grouped together with those demonstrating BRAF mutation only. Moreover, 6 additional cases presented with a BRAF duplication. In three cases, BRAF duplication was the only molecular alteration recorded, whereas in three other cases, it was associated with FGFR1 exon 16 duplication. For further analyses these 3 cases were grouped together with those demonstrating FGFR1 exon 16 duplication only.

Correlation between histopathological diagnosis, clinico-pathological and molecular data

No difference in age, sex, tumor location, and tumor recurrence was recorded between the three groups of patients (DNT, GG and GNT/PLGG). The results are summarized in Table 1.

We did not observe statistical difference regarding the pattern of growth (infiltrative *versus* nodular) within the three groups. Although calcifications were more frequent in GNT/PLGG group (15/39) than in GG (4/14) or DNT (2/19) it was not statistically significant (p = 0.084). In contrast, presence of eosinophilic granular bodies (p = 0.034), inflammation and CD34 immunostaining (p < 0.0001) were more frequent in GG group than in the two other groups. *BRAF* V600E mutation was more frequent in GG (10/14) than in GNT/PLGG (10/35) or DNT (0/19) (p < 0.0001). In contrast, occurrence of *FGFR1* mutation or duplication was not statistically different within the three groups of patients (p = 0.247). These results are summarized in Table 2. At last, extravascular CD34 expression was strongly associated with *BRAF* V600E mutation (among the 32 cases with CD34 expression, 19 displayed *BRAF* V600E mutation whereas only 1/36 cases negative for CD34 demonstrated *BRAF* V600E mutation) (p < 0.0001).

DNA methylation profiling

Results were obtained in all cases (n = 46; 64%). However only 12 cases displayed a methylation class (MC) associated with a calibrated score > 0.9 (26 %). Among them we recorded 3 cases with a MC concordant with pathological diagnosis (confirmatory), 4 cases with a MC inconsistent with pathological diagnosis (control tissue) and for 5 cases the diagnosis was refined: 5 GNT/PLGG were reclassified as LGG DNT (3 cases) (Figure 2) or LGG GG (2 cases).

Non informative calibrated score (> 0.3 and < 0.9) was observed in 26 cases (56.5%). At last in 8 cases MC score was less than 0.3 (17.5%) and no MC could be assigned.

Targeted RNA sequencing

Among the 34 cases without alteration found by mdPCR, 26 were eligible for targeted RNA sequencing. One had technical failure (FFPE block older than 8 years). Twenty-five were analyzable. A fusion transcript was found in 9 cases: one *FGFR1-TACC1*,

two *FGFR2* fusions (*FGFR2-INA* and *FGFR2-KIAA1598)* (Figure 3), two *FGFR3-TACC3* fusions (Figure 4, Supplementary Figure 1), two *BRAF* fusions (*RNF130-BRAF* and *NPM1-BRAF)*, and two *NTRK2* fusions (*KCTD16-NTRK2* and *TNS3-NTRK2*) (Supplementary Figure 1). Except for *NPM1-BRAF* fusion all other fusions have been previously reported in primitive brain tumors, with proven or predicted activation of the MAPK pathway (11,35). The results are summarized in Table 3.

Unsupervised clustering analysis based on DNA methylation data revealed two main clusters: LGG/ganglioglioma and LGG/DNT

Unsupervised hierarchical clustering based on 34 tumors (8 DNT, 5 GG and 21 GNT/PLGG) included in the present series revealed two major clusters (Figure 5). The first one comprised all the cases histologically classified as DNT as well as 2 GG and 11 GNT/PLGG, while the second one includes 3 GG and 10 GNT/PLGG. *FGFR1* alterations, recorded in 7 cases (mutation, duplication and fusion), were exclusively observed in cluster 1 whereas 7/9 cases harboring the BRAF V600E mutation were found in cluster 2. Cluster 2 was enriched in cases demonstrating CD34 expression (9/13 (%)) while only 4/21 of the cases (%) from the cluster 1 showed CD34 expression. Age and sex distribution were in similar range in both clusters. Although the temporal location was the most frequent in the whole cohort, it was obvious that large tumors and tumors located outside the temporal lobe were more frequently observed in cluster 1 (10/21, %) than in cluster 2 (3/13, %). In addition, all cases showing relapses (4 cases) were found in cluster 1. All cases (n = 15) with a max-score for the LGG DNT methylation class (range 0.33 to 0.98) fell into the cluster 1 whereas cluster 2 encompasses all cases (n = 3) with max-score >0.9 for the LGG GG methylation class as well as 4/5 cases with a low max-score for LGG GG (range 0.31-0.89). Therefore, we named cluster 1 LGG/DNT and cluster 2 LGG/GG. Importantly, the cases classified at histology as GNT/PLGG were equally distributed in the two clusters. Among the two cases classified at histology as GG and belonging to the cluster LGG/DNT, one case match with the methylation class LGG PA, subclass hemispheric PA/GG and the other showed a max score (0.86) for LGG PA. These two cases expressed CD34 and demonstrated *BRAF* V600E mutation.

Diagnostic testing algorithm for supratentorial tumors with an oligodendroglioma-like component occurring in children and young adults

According to our results we suggest the following algorithm to improve and facilitate diagnosis of supratentorial tumors with an oligodendroglioma-like component occurring in children and young adult (Figure 6). First careful pathological examination should search for GNE or DN. Tumors showing GNE can be classified as DNT and those with DN as GG. In these cases, search for molecular alteration is not required. When these pathological features are lacking it is mandatory to search for *FGFR1* mutations and/or duplication and *BRAF* V600E mutation. Cases demonstrating *FGFR1* alteration can be classified as diffuse LGG MAPK pathway-altered. In cases lacking *FGFR1* alteration and *BRAF* V600E mutation search for fusion activating MAPK pathway is required. In both cases harboring *BRAF* V600E mutation and cases demonstrating fusion, presence of calcification and CD34 expression should prompt to the diagnosis of PLNTY whereas the remaining cases fulfill criteria for diffuse LGG MAPK pathway-altered. In all cases DNA-methylation profiling might help tumor classification but it is of utmost importance to perform this technique in cases lacking GNE, dysplastic neurons and the molecular alterations described above. Moreover, DNA-methylation profiling could rule out another diagnosis. This is summarized in Figure 6.

According to our algorithm, 7/72 cases were classified as PLNTY, 16/72 as GG, 16/72 as diffuse LGG MAPK pathway altered, and 23/72 as DNT. Finally, 10/72 cases remained unconcluded because techniques could not be performed (5/10) or did not provide additional information (5/10). For these last ones, no fusion was detected, and no MC could be assigned. Indeed, one had a calibrated score < 0.3, two had a max score of respectively 0.31 and 0.32 for LGG GG MC, and two had a max score of respectively 0.64 and 0.72 for LGG DNT MC.

DISCUSSION

Glioneuronal tumors including DNT and GG are characterized by the presence of a glial component that may resemble fibrillary astrocytoma, oligodendroglioma or pilocytic astrocytoma and a neuronal component characterized by the GNE in DNT and dysplastic neurons (also named dysmorphic ganglion cells) in GG. In some cases, the glial component is made of monomorphous oligodendroglioma-like cells only. Oligodendroglioma-like component might be the unique neoplastic cells in some diffuse low-grade glioma MAPK pathway-altered and in PLNTY (14,16). These two tumor types, that will be included in the WHO CNS5 tumor classification as new entities, lack characteristic pathological features although calcifications and CD34 expression are common in PLNTY. Besides, DNT, GG, diffuse low-grade glioma MAPK pathway-activated and PLNTY belong to the group of long-term epilepsy associated tumor (LEAT) (36) and share in common, in addition to refractory epilepsy, supratentorial location, young age, indolent behavior and genetic alterations causing activation of the MAP kinase signaling pathway (14,22). Unsurprisingly, the differential diagnosis between these four tumor types remains difficult. Although DNA-methylation profiling has emerged as a powerful molecular tool to classify CNS tumors (30,31) some authors have pointed out its less accurate value to decipher challenging diagnoses among low grade glial and glioneuronal tumors (37,38). In accordance with these last studies, DNA-methylation profiling of the cases included in the present work provides disappointing results. Only 12/46 cases tested displayed a methylation class with a calibrated score of diagnostic value (>0.9) and among these, 4 cases showed a MC of control tissue. In 26 cases however, although the MC was associated with a calibrated score under the threshold value for diagnosis (<0.9), it provides consistent results for LGG and in 8 cases no MC could be assigned (calibrated score <0.3). Importantly, in none of the cases included in the present series, the MC pointed to other tumor types than LEAT tumors suggesting that the cases were accurately selected. It is likely that the low tumor cell density of the tumors analyzed as well as normal tissue included in the specimen subjected to DNA-methylation profiling might explain in part the low methylation scores observed in our series, since macrodissection was not performed. Nevertheless, in all cases the tumor represented at least 40% of the specimen. Another limitation of DNA-methylation profiling in LEAT tumors is represented by the wide range of MC for LGG tumors. In our series, four MC were observed including LGG DNT, LGG GG, LGG PA, LGG PA, subclass hemispheric PA/GG, highlighting the commonalities between

all these tumors. Moreover, there is no MC assigned yet by the 11b4 version of the Heidelberg classifier for PLNTY nor LGG MAPK pathway-activated entities. In spite of these limitations it was obvious that unsupervised clustering provides an overview of emerging subgroups among tumors. Our analysis recognized two main clusters of tumors that we named LGG/GG group and LGG/DNT group and classified all the cases diagnosed at histology as GNT/PLGG into these two main groups. This is in accordance with two previous studies focusing on LEAT tumors (26,39). In one study that comprised 43 GG, 18 DNT and 37 so called “glioneuronal tumors of uncertain histologic type” (GNT NOS) two tumor groups were recorded after DNA-methylation profiling: group 1 contained 19 GG, 1 DNT and 1 GNT NOS whereas group 2 encompasses 2 GG, 8 DNT and 6 GNT NOS (39). In the other study that included 5 DNT, 8 GG and 7 “diffuse glioneuronal tumors”, cluster 1 comprised all the DNT whereas the other tumors belonged to cluster 2 (26). Of interest one study underlined the oligodendroglioma-like component found in 11/43 GG, 17/18 DNT and 16/37 GNT NOS (39). Although it remains overlap between clinic, pathological features among the two tumor groups: LGG/GG and LGG/DNT, it is obvious that some specificities especially regarding pathogenic mutations in *BRAF* and *FGFR1* distribution occur in each group highlighting their biological relevance. The LGG/DNT group contains all tumors with a pathological diagnostic of DNT (by using strict pathological criteria) and all tumors displaying *FGFR1* alterations. Although we and others have previously reported BRAFV600E mutation in DNT (26,40,41), other studies failed to find this alteration in these tumors (15,42). These discrepant results likely rely on marked inter-observer variability in making DNT diagnosis (26,36). Among *FGFR1* alterations, duplication of the tyrosine kinase domain (TKD) is relatively unique to DNT (15,27,42). Although *FGFR1* alterations characterize the LGG/DNT group it is obvious that some typical DNT (on both pathological criteria and MC LGG DNT) are devoided of this genetic alteration. Therefore, *FGFR1* alteration is not required for DNT diagnosis but its occurrence in a supratentorial tumor with an oligodendroglioma-like component should point towards DNT and in the absence of the characteristic GNE, to the diagnosis of diffuse low-grade glioma MAPK pathway-altered (14). In contrast to *Qaddoumi et al*. who recorded *FGFR1* alteration in up to 93% (39/42) of LGG with an oligodendroglial phenotype, a large part of the cases included in the present study that share the oligodendroglioma-like component do not harbor *FGFR1* alteration and belong to the LGG/GG group (15). This group is enriched in cases demonstrating *BRAF* V600E mutation. Again this alteration is not

specific and is encountered in many tumor types (including LGG and high grade glioma) but is a common feature of GG and PLNTY (22,36). *BRAF* V600E mutation in contrast to *FGFR1* alteration is strongly associated with CD34 expression (26,39)(present study). In GNT/PLGG tumors with a major oligodendroglioma-like component, careful attention must be paid to tumors demonstrating CD34 expression and calcifications to perform a diagnosis of PLNTY. In our series 7 tumors fulfill these criteria. They include 5 cases with *BRAF* V600E mutation, and two cases with *FGFR2* fusion (*FGFR2-INA* and *FGFR2-KIAA1598*). Interestingly the present case presenting *FGFR2-INA* fusion share with the previous reported cases same pathological features: oligodendroglioma-like component, CD34 expression and calcifications (43). In the present study we also observed two cases with *FGFR3-TACC3* fusion classified at histology as GG for one and PLGG/GNT for the other. One case showed CD34 expression but no calcification and the other the reverse; therefore, they do not fulfill all criteria for a PLNTY. Importantly the case with intraventricular location displayed numerous chromosomal copy number aberrations (CNAs) and relapsed in contrast to the other. *FGFR3-TACC3* fusion has been previously reported in LGG including PLNTY (20,22,25,44), and one malignant transformation of a PLNTY is on record (44). Since *FGFR3-TACC3* also characterized a subset of malignant diffuse glioma in adults (45), we strongly encourage to follow carefully LGG harboring this fusion. In keeping with previous reports (39,41,46) we record in our series frequent CNAs, the most frequent being gains at chromosome 5 and 7. At last we recorded in our series *NPM1-BRAF* fusion which has not been previously reported in LGG. The auto-inhibitory N-terminal domain of BRAF is lacking in the predicted NPM1-BRAF fusion protein and various studies have shown that *BRAF* fusions promote MAPK pathway activation by effectuating loss of this domain (47). The *NPM1-BRAF* fusion encompasses almost all of the coding sequence of *NPM1*, coding for nucleophosmin 1, a nucleolar phosphoprotein implicated in several pathways including mRNA transport, chromatin remodeling and genome stability. Recurrent *NPM1-HAUSS1* fusions have been reported in acute myeloid leukemias with a similar breakpoint in *NPM1* exon 11 (48). To prove the oncogenicity or specificity of this new *NPM1-BRAF* fusion is beyond the scope of this descriptive study.

To conclude, our study highlights the challenges in the diagnosis of supratentorial tumors with an oligodendroglioma-like component occurring in children and young adults. It shows that these tumors belong to two major group of biological relevance

although the WHO CNS5 classification recognized four entities within this spectrum of tumors. We also suggest a step by step algorithm to achieve the histomolecular diagnosis.

FUNDING

We thank the ARTC-Sud patients' association (*Association pour le Recherche sur les Tumeurs Cérébrales*), the Association Cassandra, Liv & Lumière, the Imagine For Margo Association, the SFCE (*Société Française de Lutte contre les Cancers et Leucémies de l'Enfant et de l'Adolescent*), Enfants Cancers Santé (ECS), the Cancéropôle PACA, and the GIRCI Méditerranée (GlioMark protocol) for their financial support.

ACKNOWLEDGMENTS

We would like to thanks the AP-HM Tumor Bank (CRB-TBM, authorization number: AC2018-31053; CRB BB-0033-00097) for providing tissue samples.

REFERENCES

1. Louis DN, Ohgaki H, Wiestler OD, Cavenee WK, Ellison DW, Figarella-Branger D, et al. WHO Classification of Tumours of the Central Nervous System. 4th éd. 2016.

2. Yan H, Parsons DW, Jin G, McLendon R, Rasheed BA, Yuan W, et al. IDH1 and IDH2 mutations in gliomas. N Engl J Med. 2009;360(8):765-73.

3. Jenkins RB, Blair H, Ballman KV, Giannini C, Arusell RM, Law M, et al. A t(1;19)(q10;p10) mediates the combined deletions of 1p and 19q and predicts a better prognosis of patients with oligodendroglioma. Cancer Res. 2006;66(20):9852-61.

4. Schwartzentruber J, Korshunov A, Liu X-Y, Jones DTW, Pfaff E, Jacob K, et al. Driver mutations in histone H3.3 and chromatin remodelling genes in paediatric glioblastoma. Nature. 2012;482(7384):226-31.

5. Kreiger PA, Okada Y, Simon S, Rorke LB, Louis DN, Golden JA. Losses of chromosomes 1p and 19q are rare in pediatric oligodendrogliomas. Acta Neuropathol (Berl). 2005;109(4):387-92.

6. Raghavan R, Balani J, Perry A, Margraf L, Vono MB, Cai DX, et al. Pediatric oligodendrogliomas: a study of molecular alterations on 1p and 19q using fluorescence in situ hybridization. J Neuropathol Exp Neurol. 2003;62(5):530-7.

7. Rodriguez FJ, Tihan T, Lin D, McDonald W, Nigro J, Feuerstein B, et al. Clinicopathologic features of pediatric oligodendrogliomas: a series of 50 patients. Am J Surg Pathol. 2014;38(8):1058-70.

8. Collins VP, Jones DTW, Giannini C. Pilocytic astrocytoma: pathology, molecular mechanisms and markers. Acta Neuropathol (Berl). 2015;129(6):775-88.

9. Zhang J, Wu G, Miller CP, Tatevossian RG, Dalton JD, Tang B, et al. Whole-genome sequencing identifies genetic alterations in pediatric low-grade gliomas. Nat Genet. 2013;45(6):602-12.

10. Surrey LF, Jain P, Zhang B, Straka J, Zhao X, Harding BN, et al. Genomic Analysis of Dysembryoplastic Neuroepithelial Tumor Spectrum Reveals a Diversity of Molecular Alterations Dysregulating the MAPK and PI3K/mTOR Pathways. J Neuropathol Exp Neurol. 2019;78(12):1100-11.

11. Ryall S, Zapotocky M, Fukuoka K, Nobre L, Guerreiro Stucklin A, Bennett J, et al. Integrated Molecular and Clinical Analysis of 1,000 Pediatric Low-Grade Gliomas. Cancer Cell. 2020;37(4):569-583.e5.

12. Louis DN, Aldape K, Brat DJ, Capper D, Ellison DW, Hawkins C, et al. cIMPACT-NOW (the consortium to inform molecular and practical approaches to CNS tumor taxonomy): a new initiative in advancing nervous system tumor classification. Brain Pathol. 2017;27(6):851-2.

13. Brat DJ, Aldape K, Colman H, Holland EC, Louis DN, Jenkins RB, et al. cIMPACT-NOW Update 3: Recommended diagnostic criteria for “Diffuse

astrocytic glioma, IDH-wildtype, with molecular features of glioblastoma, WHO grade IV". Acta Neuropathol (Berl). 2018;136(5):805-10.

14. Ellison DW, Hawkins C, Jones DTW, Onar-Thomas A, Pfister SM, Reifenberger G, et al. cIMPACT-NOW update 4: diffuse gliomas characterized by MYB, MYBL1, or FGFR1 alterations or BRAFV600E mutation. Acta Neuropathol (Berl). 2019;137(4):683-7.

15. Qaddoumi I, Orisme W, Wen J, Santiago T, Gupta K, Dalton JD, et al. Genetic alterations in uncommon low-grade neuroepithelial tumors: BRAF, FGFR1, and MYB mutations occur at high frequency and align with morphology. Acta Neuropathol (Berl). 2016;131(6):833-45.

16. Louis DN, Wesseling P, Aldape K, Brat DJ, Capper D, Cree IA, et al. cIMPACT-NOW update 6: new entity and diagnostic principle recommendations of the cIMPACT-Utrecht meeting on future CNS tumor classification and grading. Brain Pathol. 2020;30(4):844-56.

17. Bandopadhayay P, Ramkissoon LA, Jain P, Bergthold G, Wala J, Zeid R, et al. MYB-QKI rearrangements in angiocentric glioma drive tumorigenicity through a tripartite mechanism. Nat Genet. 2016;48(3):273-82.

18. Chiang J, Harreld JH, Tinkle CL, Moreira DC, Li X, Acharya S, et al. A single-center study of the clinicopathologic correlates of gliomas with a MYB or MYBL1 alteration. Acta Neuropathol (Berl). 2019;138(6):1091-2.

19. Wefers AK, Stichel D, Schrimpf D, Coras R, Pages M, Tauziède-Espariat A, et al. Isomorphic diffuse glioma is a morphologically and molecularly distinct tumour entity with recurrent gene fusions of MYBL1 or MYB and a benign disease course. Acta Neuropathol (Berl). 2020;139(1):193-209.

20. Gupta VR, Giller C, Kolhe R, Forseen SE, Sharma S. Polymorphous Low-Grade Neuroepithelial Tumor of the Young: A Case Report with Genomic Findings. World Neurosurg. 2019;132:347-55.

21. Hewer E, Knecht U, Ulrich CT. Two adult cases of massively calcified low-grade glioma: expanding clinical spectrum of an emerging entity. Neuropathology. 2016;36(5):508-9.

22. Huse JT, Snuderl M, Jones DTW, Brathwaite CD, Altman N, Lavi E, et al. Polymorphous low-grade neuroepithelial tumor of the young (PLNTY): an epileptogenic neoplasm with oligodendroglioma-like components, aberrant CD34 expression, and genetic alterations involving the MAP kinase pathway. Acta Neuropathol (Berl). 2017;133(3):417-29.

23. Riva G, Cima L, Villanova M, Ghimenton C, Sina S, Riccioni L, et al. Low-grade neuroepithelial tumor: Unusual presentation in an adult without history of seizures. Neuropathology. 2018;38(5):557-60.

24. Sumdani H, Shahbuddin Z, Harper G, Hamilton L. Case Report of Rarely Described Polymorphous Low-Grade Neuroepithelial Tumor of the Young and Comparison with Oligodendroglioma. World Neurosurg. 2019;127:47-51.

25. Bitar M, Danish SF, Rosenblum MK. A newly diagnosed case of polymorphous low-grade neuroepithelial tumor of the young. Clin Neuropathol. 2018;37(4):178-81.

26. Blumcke I, Coras R, Wefers AK, Capper D, Aronica E, Becker A, et al. Review: Challenges in the histopathological classification of ganglioglioma and DNT: microscopic agreement studies and a preliminary genotype-phenotype analysis. Neuropathol Appl Neurobiol. 2019;(2):95.

27. Fina F, Barets D, Colin C, Bouvier C, Padovani L, Nanni-Metellus I, et al. Droplet digital PCR is a powerful technique to demonstrate frequent FGFR1 duplication in dysembryoplastic neuroepithelial tumors. Oncotarget. 2017;8(2):2104-13.

28. Appay R, Fina F, Macagno N, Padovani L, Colin C, Barets D, et al. Duplications of KIAA1549 and BRAF screening by Droplet Digital PCR from formalin-fixed paraffin-embedded DNA is an accurate alternative for KIAA1549-BRAF fusion detection in pilocytic astrocytomas. Mod Pathol. 2018;31(10):1490.

29. Appay R, Fina F, Barets D, Gallardo C, Nanni-Metellus I, Scavarda D, et al. Multiplexed Droplet Digital PCR Assays for the Simultaneous Screening of Major Genetic Alterations in Tumors of the Central Nervous System. Front Oncol. 2020;10:579762.

30. Capper D, Stichel D, Sahm F, Jones DTW, Schrimpf D, Sill M, et al. Practical implementation of DNA methylation and copy-number-based CNS tumor diagnostics: the Heidelberg experience. Acta Neuropathol (Berl). 2018;136(2):181-210.

31. Capper D, Jones DTW, Sill M, Hovestadt V, Schrimpf D, Sturm D, et al. DNA methylation-based classification of central nervous system tumours. Nature. 2018;555(7697):469-74.

32. Siegfried A, Rousseau A, Maurage C-A, Pericart S, Nicaise Y, Escudie F, et al. EWSR1-PATZ1 gene fusion may define a new glioneuronal tumor entity. Brain Pathol. 2019;(1):53.

33. Dobin A, Davis CA, Schlesinger F, Drenkow J, Zaleski C, Jha S, et al. STAR: ultrafast universal RNA-seq aligner. Bioinformatics. 2013;29(1):15-21.

34. Chen X, Schulz-Trieglaff O, Shaw R, Barnes B, Schlesinger F, Källberg M, et al. Manta: rapid detection of structural variants and indels for germline and cancer sequencing applications. Bioinformatics. 2016;32(8):1220-2.

35. Jones DTW, Hutter B, Jäger N, Korshunov A, Kool M, Warnatz H-J, et al. Recurrent somatic alterations of FGFR1 and NTRK2 in pilocytic astrocytoma. Nat Genet. 2013;45(8):927-32.

36. Blümcke I, Aronica E, Becker A, Capper D, Coras R, Honavar M, et al. Low-grade epilepsy-associated neuroepithelial tumours - the 2016 WHO classification. Nat Rev Neurol. 2016;12(12):732-40.

37. Pickles JC, Fairchild AR, Stone TJ, Brownlee L, Merve A, Yasin SA, et al. DNA methylation-based profiling for paediatric CNS tumour diagnosis and treatment: a population-based study. Lancet Child Adolesc Health. 2020;4(2):121-30.

38. Pages M, Uro-Coste E, Colin C, Meyronet D, Gauchotte G, Maurage C-A, et al. The implementation of DNA methylation profiling into a multistep diagnostic process in pediatric neuropathology: A 2-years real world experience by the French Neuropathology Network. Cancers. 2021;13(1377).

39. Stone TJ, Keeley A, Virasami A, Harkness W, Tisdall M, Izquierdo Delgado E, et al. Comprehensive molecular characterisation of epilepsy-associated glioneuronal tumours. Acta Neuropathol (Berl). 2018;135(1):115-29.

40. Chappe C, Padovani L, Scavarda D, Forest F, Nanni-Metellus I, Loundou A, et al. Dysembryoplastic Neuroepithelial Tumors Share with Pleomorphic Xanthoastrocytomas and Gangliogliomas BRAFV600E Mutation and Expression. Brain Pathol. 2013;(5):574.

41. Prabowo AS, Iyer AM, Veersema TJ, Anink JJ, Schouten-van Meeteren AYN, Spliet WGM, et al. BRAF V600E Mutation Is Associated with mTOR Signaling Activation in Glioneuronal Tumors. Brain Pathol. 2014;(1):52.

42. Matsumura N, Nobusawa S, Ito J, Kakita A, Suzuki H, Fujii Y, et al. Multiplex ligation-dependent probe amplification analysis is useful for detecting a copy number gain of the FGFR1 tyrosine kinase domain in dysembryoplastic neuroepithelial tumors. J Neurooncol. 2019;143(1):27-33.

43. Jain P, Surrey LF, Straka J, Luo M, Lin F, Harding B, et al. Novel FGFR2-INA fusion identified in two low-grade mixed neuronal-glial tumors drives oncogenesis via MAPK and PI3K/mTOR pathway activation. Acta Neuropathol (Berl). 2018;136(1):167-9.

44. Bale TA. FGFR- gene family alterations in low-grade neuroepithelial tumors. Acta Neuropathol Commun. 2020;8(1):1-9.

45. Bielle F, Di Stefano A-L, Meyronet D, Picca A, Villa C, Bernier M, et al. Diffuse gliomas with FGFR3-TACC3 fusion have characteristic histopathological and molecular features. Brain Pathol. 2018;(5):674.

46. Li Y, Wang D, Wang L, Yu J, Du D, Chen Y, et al. Distinct Genomic Aberrations between Low-Grade and High-Grade Gliomas of Chinese Patients. PLoS ONE [Internet]. 2013 [cité 1 avr 2021];8(2). Disponible sur: https://www.ncbi.nlm.nih.gov/pmc/articles/PMC3579804/

47. Stangl C, Post JB, van Roosmalen MJ, Hami N, Verlaan-Klink I, Vos HR, et al. Diverse BRAF Gene Fusions Confer Resistance to EGFR-Targeted Therapy via Differential Modulation of BRAF Activity. Mol Cancer Res MCR. 2020;18(4):537-48.

48. Campregher PV, de Oliveira Pereira W, Lisboa B, Puga R, Deolinda ERPV, Helman R, et al. A novel mechanism of NPM1 cytoplasmic localization in acute myeloid leukemia: the recurrent gene fusion NPM1-HAUS1. Haematologica. 2016;101(7):e287-290.

TABLES

Clinical features	DNET	GG	GNT/PLGG
Gender (*n* = 72)	12M/7F	9M/5F	22M/17F
Age at surgery (years) **(*n* = 72)**	13.3 [4.0 -32.9] (*n* = 19)	14.8 [0.3-36.6] (*n* = 14)	14 [0.8-57.2] (n = *39*)
Tumor location **(*n* = 72)**	Frontal (*n* = 6) Temporal (*n* = 10) Other (*n* = 3)	Frontal (*n* = 1) Temporal (*n* = 12) Other (*n* = 1)	Frontal (*n* = 5) Temporal (*n* = 22) Other (*n* = 12)
Recurrence **(*n* = 63)**	1 (*n* = 16)	2 (*n* = 14)	6 (*n* = 33)
Median time between first surgery and recurrence (months) **(*n* = 9)**	126.9 (*n* = 1)	160.5 [107.7-213.3] (*n* = 2]	52.6 [5.3-70.0] (*n* = 6)
Median follow-up (months) **(*n* = 62)**	36.9 [0.1-126.9] (*n* = 16)	35.7 [2.3-229.4] (*n* = 14)	22 [0-126.3] 23 (*n* = 32)

Table 1: Summary of clinical features

DNT: dysembryoplastic neuroepithelial tumor; GG: ganglioglioma; GNT/PLGG: glioneuronal tumor / peadiatric type low-grade glioma; M: male; F: female

Histological and molecular features	DNET (*n* = 19)	GG (*n* = 14)	GNT/PLGG (*n* = 39)	Fisher exact test *p* value
Specific glioneuronal element	100% (19)	0% (0)	0% (0)	***p* < 0.0001**
Dysplastic neurons	0% (0)	100% (14)	0% (0)	***p* < 0.0001**
Infiltrative growth pattern	37% (7)	78% (11)	56% (22)	*p* = 0.059
Nodular growth pattern	63% (12)	21% (3)	44% (17)	*p* = 0.059
Calcification	11% (2)	29% (4)	38% (15)	*p* = 0.084
Eosinophilic granular bodies	5% (1)	43% (6)	23% (9)	***p* = 0.033**
Inflammation	0% (0)	57% (8)	15% (6)	***p* < 0.0001**
CD34 extravascular immunostaining	11% (2)	86% (12)	49% (19)	***p* < 0.0001**
BRAFV600E mutation	0% (0)	71% (10)	26% (10)	***p* < 0.0001**
FGFR1 alterations (mutation + duplication)	42% (8)	7% (1)	23% (9)	*p* = 0.247
FGFR1 mutation	21% (4)	0% (0)	2% (1)	*p* = 0.103
FGFR1 duplication	26% (5)	14% (2)	21% (8)	*p* = 1.000
Fusion transcript	0	1	8	

Table 2: Summary of histological and molecular features

DNT: dysembryoplastic neuroepithelial tumor; GG: ganglioglioma; GNT/PLGG: glioneuronal tumor / peadiatric type low-grade glioma

Transcript fusion	BP partner A	BP partner B	Diagnosis	Age at diagnosis (years)	Tumor location	Growth Pattern	Calcifications	Eosinophilic granular bodies	Inflammation	CD34	Recurrence	Follow-up (months)
FGFR1-TACC1	**exon 17**	**exon 2**	GNT/PLGG	4.6	Temporal	Nodular	-	-	+	-	-	21.6
NPM1-BRAF	**exon 7**	**exon 11**	GNT/PLGG	5.9	Occipital	Infiltrative	-	-	-	-	NA	NA
RNF130-BRAF	**exon 3**	**exon 9**	GNT/PLGG	11.3	Temporal	Nodular	+	-	-	-	-	3.5
FGFR2-KIAA1598	**exon 16**	**exon 7**	GNT/PLGG	9.2	Parietal	Nodular	+	+	-	+	NA	NA
FGFR2-INA	**exon 17**	**exon 2**	GNT/PLGG	3.1	Temporal	Infiltrative	+	-	-	+	+	46.9
FGFR3-TACC3	**exon 17**	**exon 12**	GG	*14.8*	Temporal	Infiltrative	-	-	-	+	-	37.9
FGFR3-TACC3	**exon 17**	**exon 10**	GNT/PLGG	*5.1*	Intraventricular	Infiltrative	+	-	-	-	+	125.5
TNS3-NTRK2	**exon 17**	**exon 10**	GNT/PLGG	44	Temporal	Infiltrative	-	-	-	-	-	0
KCTD16-NTRK2	**exon 3**	**exon 14**	GNT/PLGG	5.6	Frontal	Nodular	-	-	-	-	+	69.1

Table 3: Clinical and histological features of patients presenting with a fusion transcript

GG: ganglioglioma; GNT/PLGG: glioneuronal tumor / peadiatric type low-grade glioma; NA: not available.

FIGURES

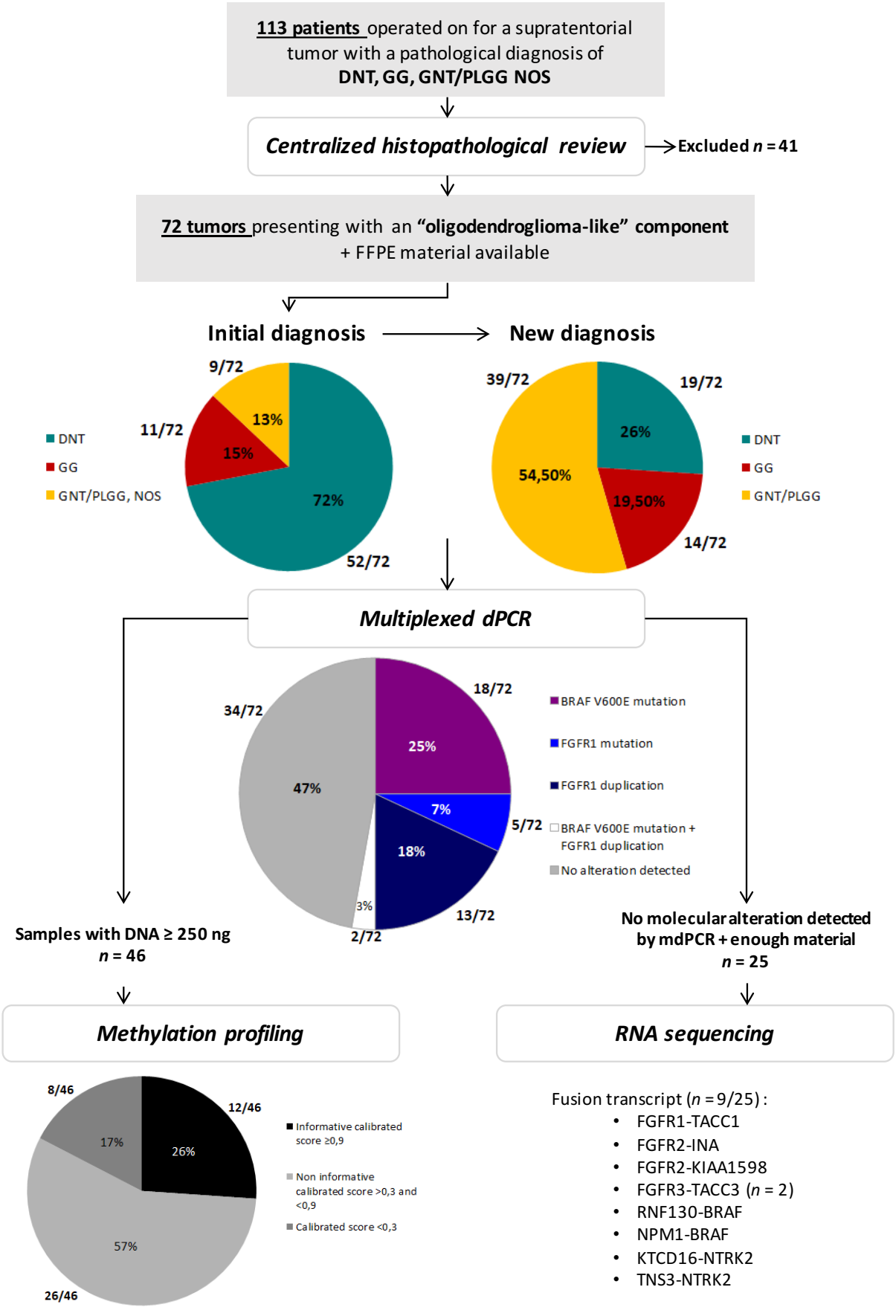

Figure 1: Workflow of the study

Figure 1: ddPCR: digital droplet PCR; DNT: dysembryoplastic neuroepithelial tumor; FFPE: formalin-fixed paraffin embedded; GG: ganglioglioma; GNT/PLGG NOS: glioneuronal tumor / paediatric type low-grade glioma not otherwise specified; GNT/PLGG: glioneuronal tumor / peadiatric type low-grade glioma; mddPCR: multiplexed digital droplet PCR.

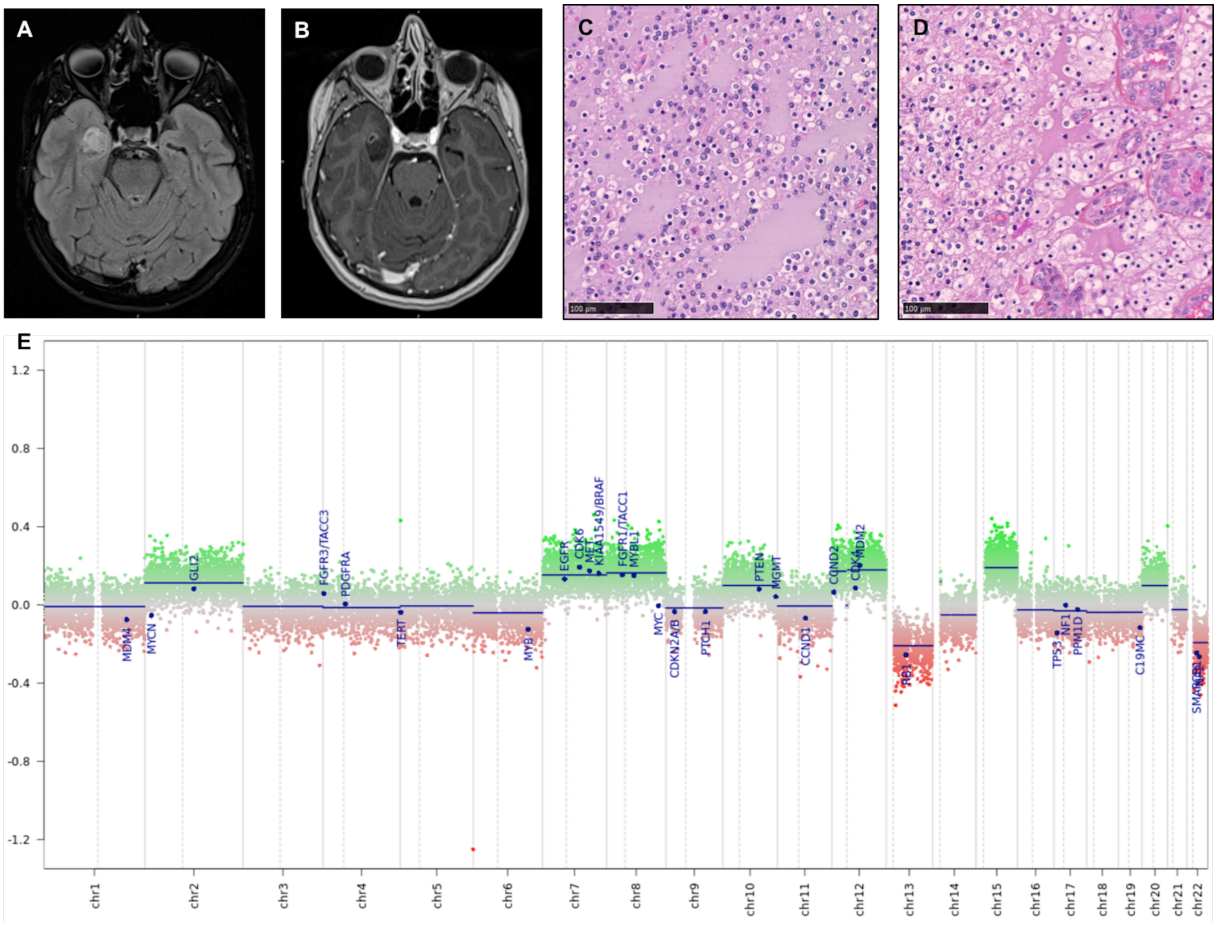

Figure 2: Tumor from a 14 years old female patient, without genetic alteration detected, with a final diagnosis of DNT after DNA-methylation profiling.

The tumor was located in the right temporal lobe and displayed bubbly cystic changes on MRI, associated with focal contrast enhancement (A: FLAIR MRI section, B: T1 with gadolinium injection). Histologically, there was an oligodendroglial-like component associated with pools of mucin without floating neurons (C: HPS section, scale bar: 100µm). Vasculature showed microvascular proliferation (D: HPS section, scale bar: 100 µm). Methylation profiling classified the tumor in LGG DNT with a calibrated score of 0.96. CNV profile was imbalanced (E: CNV plots).

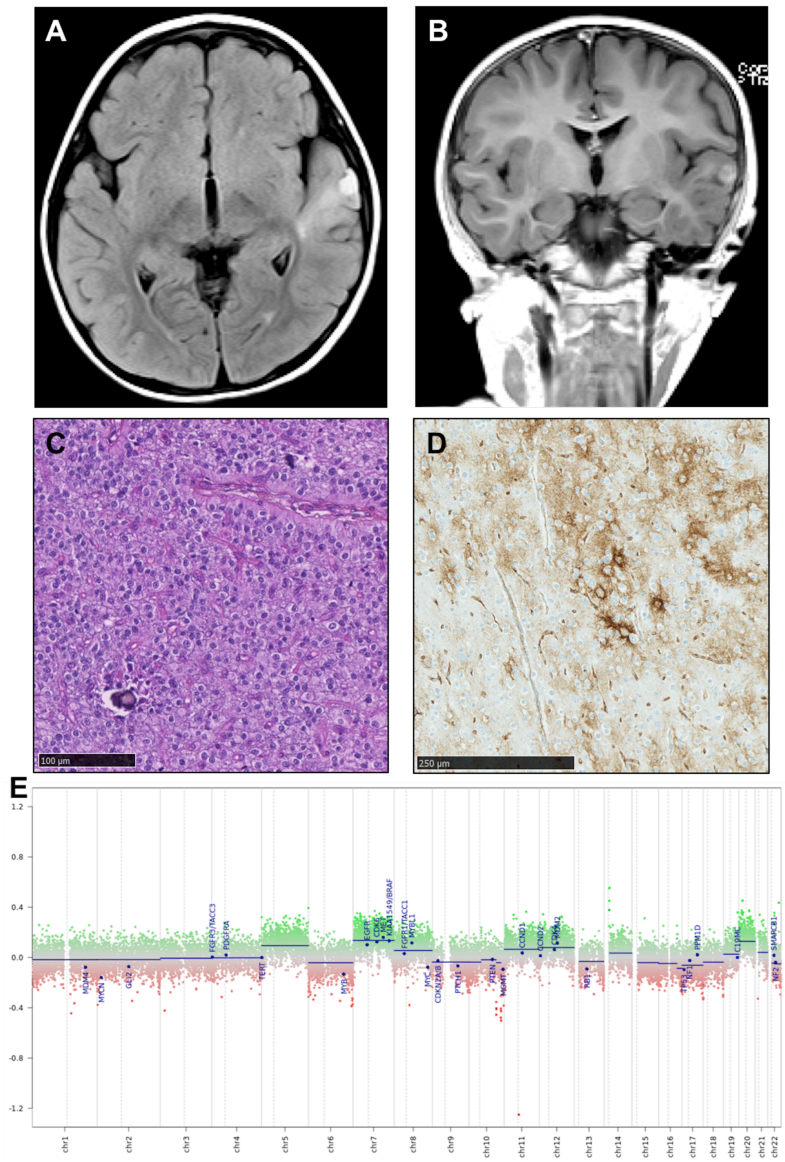

Figure 3: Tumor from a 3 years old female patient, with *FGFR2-INA* fusion, definitively classified as PLNTY.

The tumor was peripherally located in the left temporal lobe, appearing in high signal FLAIR with a nodular contrast enhancement (A: FLAIR MRI section, B: T1 with gadolinium injection). Histologically, there was oligodendroglioma-like with microcalcifications (C: HPS section, scale bar: 100µm), and extravascular CD34 expression (D: CD34 immunostaining, scale bar: 250µm). Although methylation profiling classified this tumor as LGG GG, with a calibrated score of 0.96, we classified the case as PLNTY in the absence of dysplastic neurons. CNV profile was imbalanced (E: CNV plots).

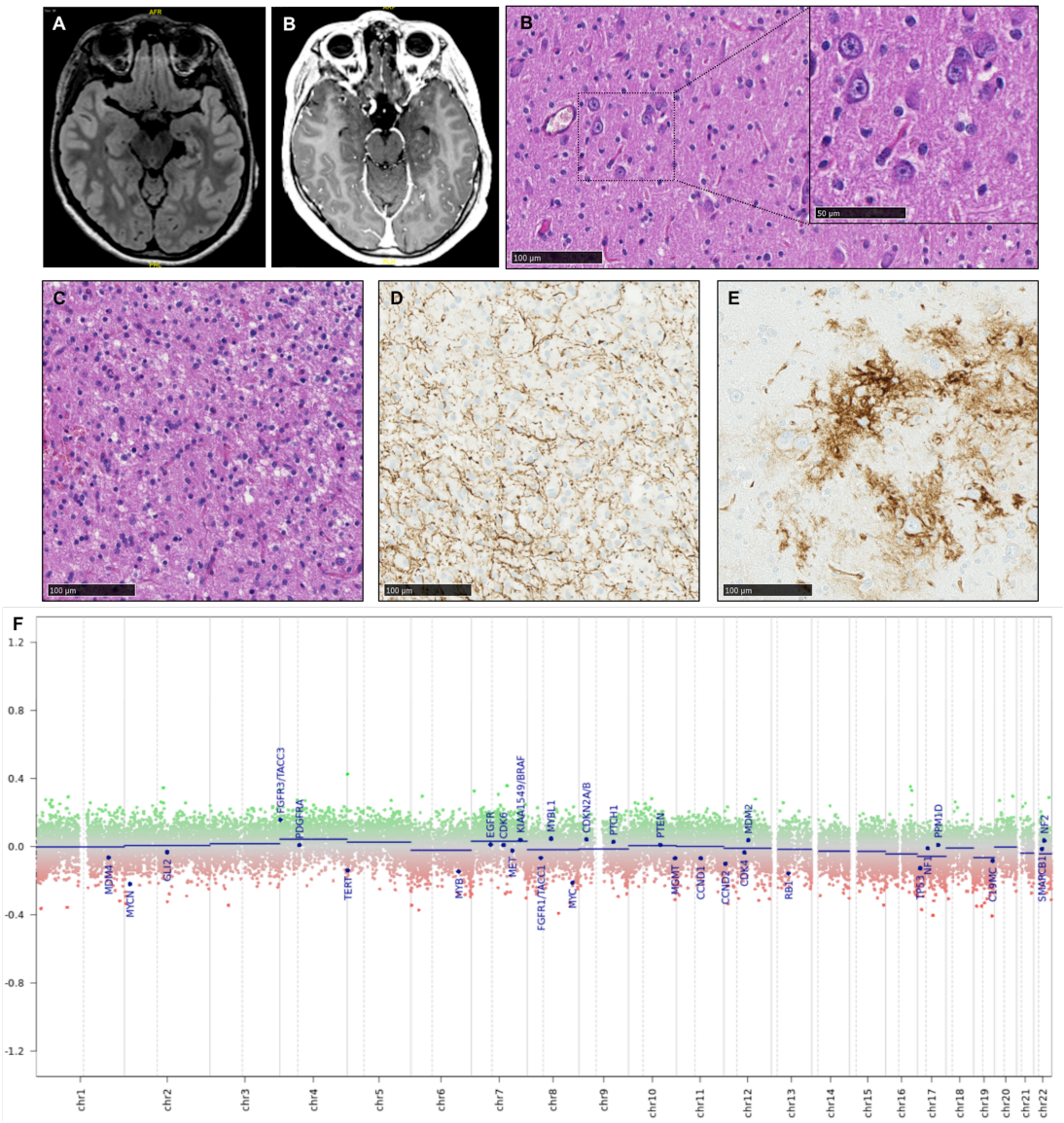

Figure 4: Tumor from a 15 years old male patient, classified as GG associated with a *FGFR3-TACC3* fusion.

The tumor was located in the right temporal lobe, displaying bubbly cystic changes and focal contrast enhancement (A: FLAIR MRI section, B: T1 with gadolinium injection). Histologically, the tumor demonstrated dysplastic neurons (B: HPS section, scale bar: 100 µm and 50 µm in the zoom box) an oligodendroglioma-like component (C: HPS section, scale bar: 100 µm). Immunohistochemistry highlighted an infiltrative growth pattern (D: neurofilament immunostaining, scale bar: 100 µm) and demonstrated extravascular CD34 immunostaining (E: CD34 immunostaining, scale bar: 100 µm). Methylation profiling classified the tumor as LGG GG with a calibrated score of 0.89. CNV profile was balanced (F: CNV plots).

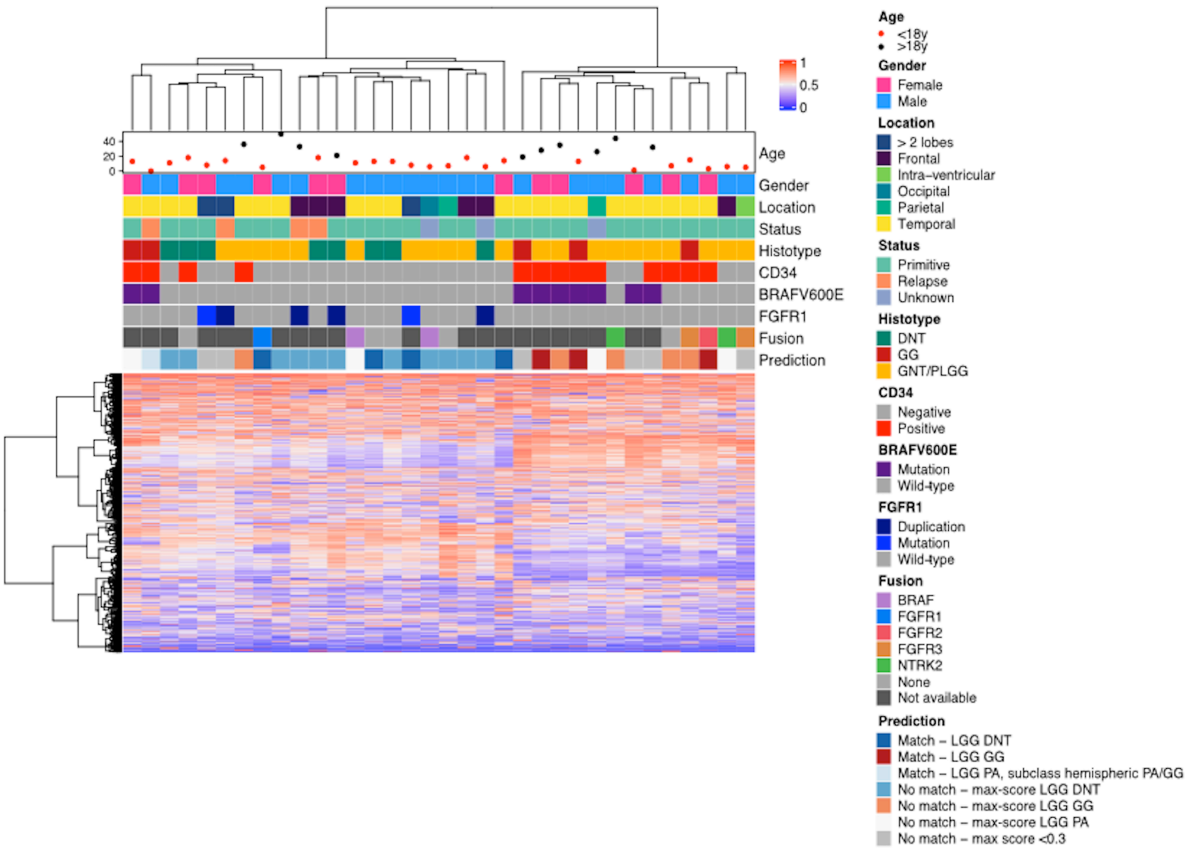

Figure 5: Unsupervised hierarchical clustering

Unsupervised hierarchical clustering revealed two groups. The first one, named LGG/DNT, was enriched in cases classified at histology as DNT (except for 2 GG), CD34 negativity and *FGFR1* alterations. The second one, named LGG/GG, was enriched for cases classified at histology as GG, CD34 positivity and *BRAF*V600E mutation.

DNT: dysembryoplastic neuroepithelial tumor; GG: ganglioglioma; GNT/PLGG: glioneuronal tumor/paediatric-type low-grade glioma; LGG DNT: methylation class low-grade glioma, dysembryoplastic neuroepithelial tumor; LGG GG: methylation class low-grade-glioma, ganglioglioma; LGG PA: methylation class low-grade glioma, pilocytic astrocytoma; LGG PA, subclass hemispheric PA/GG: methylation class low-grade-glioma, pilocytic astrocytoma, subclass hemispheric pilocytic astrocytoma/ganglioglioma.

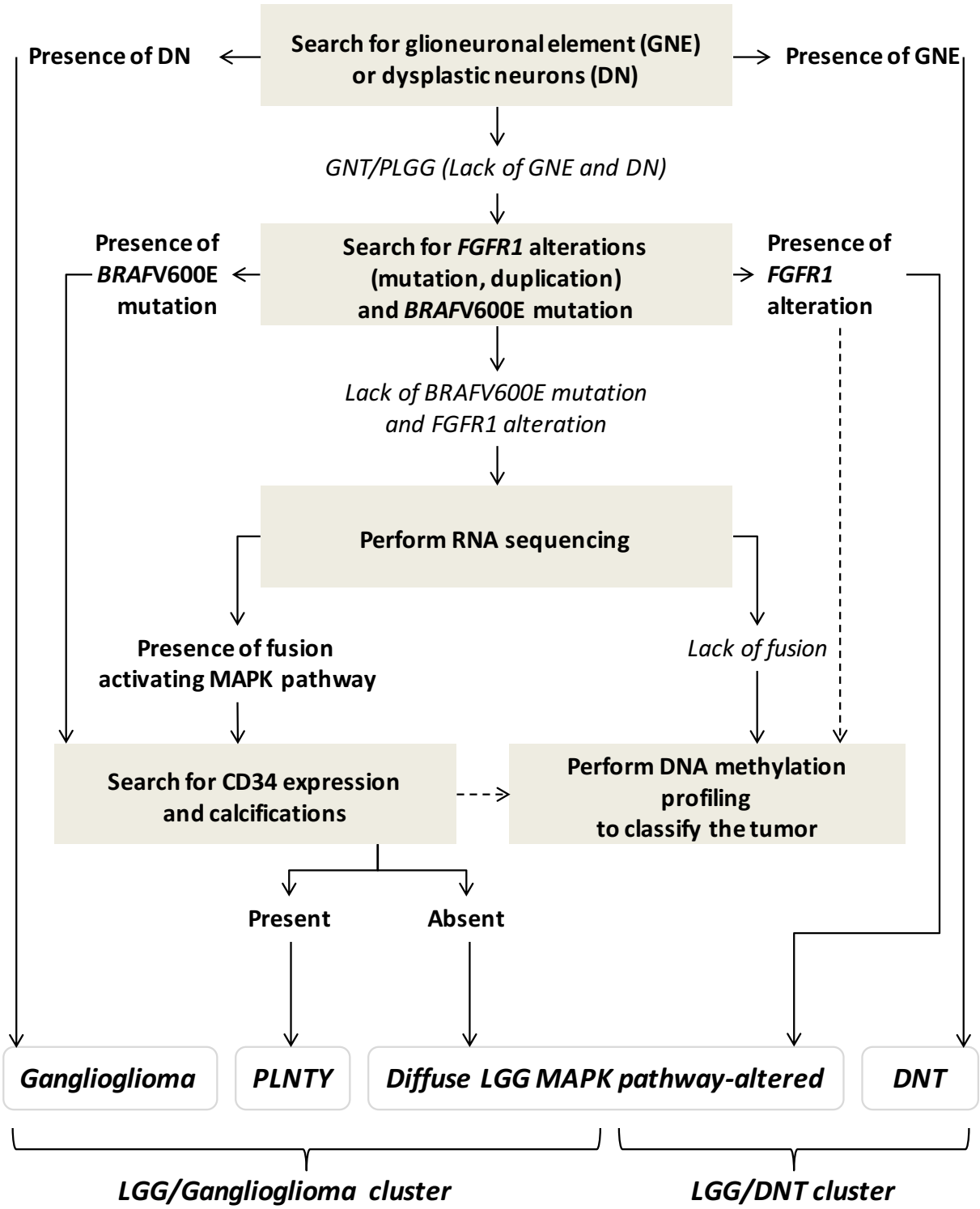

Figure 6: Proposed decision tree

DN: dysplastic neurons; DNT: dysembryoplastic neuroepithelial tumor; GNE: specific glioneuronal element; LGG: low-grade glioma; LGG/DNT: low-grade glioma/dysembryoplastic neuroepithelial tumor; PLNTY: polymorphous low-grade neuroepithelial tumor of the young.

SUPPLEMENTARY FIGURES

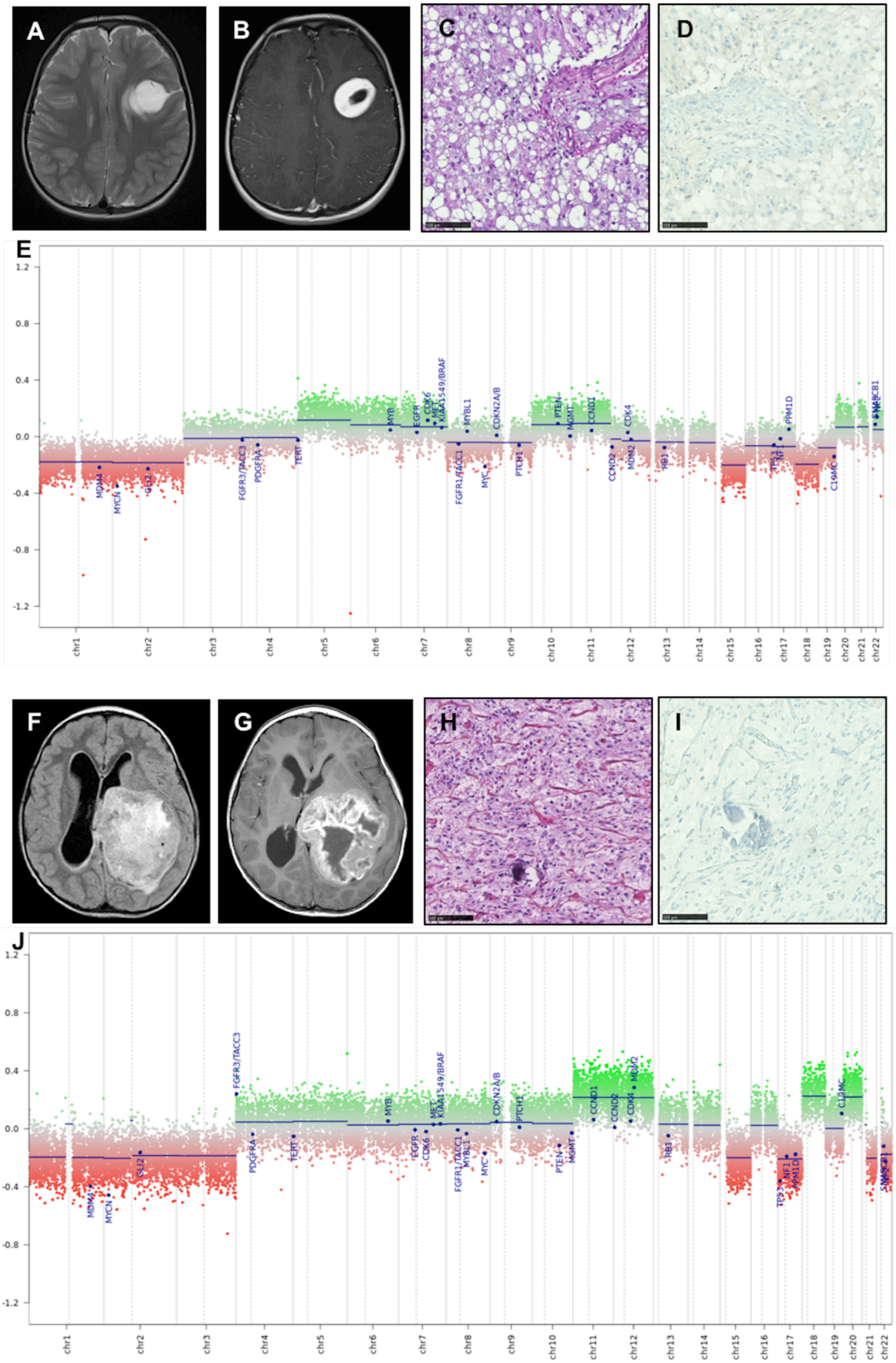

Supplementary figure 1: Cases of a 3 years old male with a *KCTD16-NTRK2* fusion (A-E) and a 5 years old male with a *FGFR3-TACC3* fusion (F-J), both definitively classified as diffuse MAPK pathway altered gliomas.

Supplementary figure 1: For the first case (A-E), the tumor was located in the left frontal cortex with contrast enhancement (A: FLAIR MRI section; B: T1 with gadolinium injection MRI section). At histology, there was a circumscribed oligodendroglioma-like lesion with massive calcifications (C: HPS section, scale bar: 100 µm; D: neurofilament immunostaining, scale bar: 100 µm) and negative for CD34 (not shown). Methylation profiling found a max score of 0,55 for LGG PA methylation class. CNV profile was imbalanced (E: CNV plots). The second case (F-J) presented as a massive intraventricular tumor, partially cystic with contrast enhancement (F: FLAIR MRI section, G: T1 with gadolinium injection MRI section). At histology there was a circumscribed oligodendroglioma-like lesion with microcalcifications and a hyaline stroma (H: HPS section, scale bar: 100 µm; I: neurofilament immunostaining, scale bar: 100 µm) and CD34 immunostaining was negative (not shown). Methylation profiling could not assign a methylation class (calibrated score < 0.3). CNV was imbalanced (J: CNV plots).

U.F.R. DE **MEDECINE** DE RENNES

N° 40-2021-

METAIS, Alice – Challenges in the diagnosis of supratentorial tumors with an oligodendroglioma-like component occuring in children and young adults

45 feuilles., 7 illustrations., 3 tableaux, 30 cm.- Thèse : (Médecine) ; Rennes 1; 2021 ; N° .

Les gliomes diffus de bas grade de sous-type pédiatrique (PLGG) et les tumeurs glioneuronales (GNT) atteignent préférentiellement les enfants et les jeunes adultes et sont à l'origine d'une épilepsie pharmaco-résistante. Histologiquement ces tumeurs sont souvent caractérisées par la présence d'un contingent glial « oligo-like », en particulier dans les gangliogliomes (GG), les tumeurs dysembryoplasiques neuro-épithéliales (DNT) ainsi que dans deux entités récemment décrites : les tumeurs neuro-épithéliales polymorphes du sujet jeune (polymorphous neuroepithelial tumor of the young, PLNTY) et les gliomes diffus de bas grade avec altération des MAPK kinases. De plus ces tumeurs ont en commun des altérations moléculaires activatrices de la voie des MAPK kinases. De part ces caractères communs les PLGG et GNT sont particulièrement difficiles à classer. Dans le but de mieux caractériser ces tumeurs, nous avons réalisé une étude rétrospective multicentrique portant sur 72 prélèvements chirurgicaux et biopsiques de tumeurs gliales et glio-neuronales de localisation supratentorielle de bas grade réalisés entre 2002 et 2020. Dans tous les cas une relecture anatomopathologique centralisée a permis de classer ces tumeurs en trois grands groupes : DNT (présence d'une composante glioneuronale spécifique, n = 19), GG (présence de cellules ganglionnaires dysplasiques, n = 14) et GNT/PLGG (n = 39). Trente-huit cas sur les 72 analysés présentait une altération moléculaire détectée par PCR digitale multiplexe (mdPCR) (mutation *BRAF*V600E, mutations et duplication de *FGFR1*). Parmi les cas 34 cas ne présentant pas d'altération, 9/26 avaient un transcrit de fusion détecté par RNAseq. Quarante-six cas ont pu être analysés par profil de méthylation, parmi lesquels 12 avaient un score de méthylation supérieur à 0,9 (26%). Un score non informatif (entre 0,9 et 0,3) était retrouvé dans 26 cas (56,5%). Pour 8 cas le score de méthylation était inférieur à 0,3 (17,5%). Le clustering hiérarchique non supervisé a montré l'existence de deux groupes entre lesquels les GNT/PLGG se répartissaient équitablement. Le groupe LGG/GG réunissait la plupart des tumeurs classées histologiquement en GG, avec une mutation *BRAF*V600E, une positivité du CD34 et dont le profil de méthylation répondait à la classe de méthylation LGG GG. Le groupe LGG/DNT réunissait les DNT, avec altération de *FGFR1*, une négativité du CD34 et répondant à la classe de méthylation LGG DNT. Sept cas ont été reclassés en PLNTY. La démarche diagnostique a été résumée dans un algorithme.

Cette étude souligne la difficulté à bien classer les tumeurs supratentorielles oligo-like chez les sujets jeunes. Enfin, bien que quatre entités soient actuellement définies pour ce type de tumeurs par la 5ème classification de l'OMS, nos résultats indiquent qu'elles se répartissent en deux groupes biologiquement distincts.

Rubrique de classement : ANATOMIE ET CYTOLOGIE PATHOLOGIQUES

Mots-clés : paediatric-type low-grade glioma, glioneuronal tumor, dysembryoplastic neuroepithelial tumor, polymorphous low-grade neuroepithelial tumor of the young, diffuse glioma MAPK pathway altered, long-term epilepsy associated tumor

Mots-clés anglais MeSH : paediatric-type low-grade glioma, glioneuronal tumor, dysembryoplastic neuroepithelial tumor, polymorphous low-grade neuroepithelial tumor of the young, diffuse glioma MAPK pathway altered, long-term epilepsy associated tumor

Président : Mme le Professeur Nathalie RIOUX-LECLERCQ

JURY : Assesseurs : Mme le Professeur Dominique FIGARELLA-BRANGER (directeur de thèse)
Mme le Professeur Pascale VARLET
Mme le Professeur Audrey ROUSSEAU
Mr le Professeur Laurent RIFFAUD
Mr Pierre-Jean LE RESTE